

Spatiotemporally Separable Biphoton State Generated by Spontaneous Four Wave Mixing in Ultrathin Nonlinear Films

Chenzhi Yuan ^{1,2}, Wei Zhang ^{1,2*}, and Yidong Huang ^{1,2}

1) *Beijing National Research Center for Information Science and Technology (BNRist), Beijing Innovation Center for Future Chips, Electronic Engineering Department, Tsinghua University, Beijing 100084, China*

2) *Beijing Academy of Quantum Information Sciences, Beijing 100193, China*

[*zwei@tsinghua.edu.cn](mailto:zwei@tsinghua.edu.cn)

We theoretically investigated the biphoton state generated by spontaneous four wave mixing (SpFWM) in ultrathin nonlinear films. The expression of the biphoton state is obtained by perturbation method, in which the longitudinal phase mismatch term is eliminated due to the ultra-small nonlinear interactive length. As a result of the relaxation of the longitudinal phase match condition, frequency bandwidth of the biphoton state could be very large. The correlation function of the biphoton state is analyzed, showing that the space and time in the biphoton correlation of this state are factorable. The calculations of the frequency purity further indicate that the temporal and spatial degrees of freedom in this biphoton state are separable. The spatial Schmidt numbers of the biphoton state are also calculated, showing that this state supports high dimensional transverse entanglement. These results show that SpFWM in ultrathin nonlinear films is promising in generating biphoton states for applications involving hyper-entanglement and high-dimensional entanglement.

I. Introduction

Spontaneous parametric nonlinear optical processes, including spontaneous parametric down conversion (SPDC) [1, 2] and spontaneous four wave mixing (SpFWM) [3-5], are important ways to generate correlated biphoton states, which have been widely investigated and applied in various experiments of quantum information processing [6] and quantum communications [7, 8] involving photons. In these processes, the energy and momentum conservations between the annihilated and generated photons determine the properties of quantum correlation in the biphoton states [9-19]. The momentum conservation can be expressed by the phase matching conditions, which is largely determined by the geometrical structure of the nonlinear media.

Usually, nonlinear optical bulk crystals [13] or periodically poled waveguides [20] with length of \sim mm are employed in SPDC. Due to the considerable interaction length, the longitudinal phase mismatch becomes remarkable and brings some limits to the generated biphoton states. For example, in these states the temporal and spatial degrees of freedom are not separable, limiting their applications in realization of hyper-entanglements [21]. It also leads to the difficulty on the definitions of temporal and spatial coherences in these states. Instead, the coherence of these states is defined in an “X” trajectory in the spatial and temporal dimensions [10, 15-16]. On the other hand, the longitudinal phase mismatch also limits the frequency and spatial frequency bandwidths of the biphoton states [12], which are important for quantum metrology techniques based on biphoton interferences [22, 23]. For the biphoton state generation by SpFWM, usually the third order nonlinear waveguides, such as optical fibers [3] and silicon waveguides [4], are employed. Long waveguide lengths are required (several hundreds meters for optical fibers and several millimeters for silicon waveguides) to compensate the low third order nonlinearity in these materials. Hence, the longitudinal phase mismatch is also important. It mainly impacts on the frequency bandwidth of the biphoton states if the processes are stimulated only in a specific waveguide mode, or among several known modes [24].

Recently, nonlinear optical effects in nonlinear thin films attracted much attention. The thicknesses of these nonlinear

films are very small, which relax the requirement of longitudinal phase matching. It has been demonstrated by four wave mixing in thin metallic films and graphite thin films [25, 26]. It also has been proposed that the longitudinal phase matching factor can be eliminated in biphoton states generated by SPDC in thin films [27]. However, properties of the biphoton state generated in the nonlinear films by either SPDC or SpFWM have not been investigated. Ref. [28] pointed out that the spatial mode analysis of biphoton states generated by SPDC would have problems of divergence if the phase matching factor disappears. It can be expected that similar problems also exists in analyzing other properties of the biphoton states generated by spontaneous parametric optical processes in thin films, such as correlation function and transverse entanglement.

In this work, we theoretically investigated the properties of biphoton states generated by SpFWM in ultrathin nonlinear films comprehensively. The expression of the biphoton state is obtained by perturbation method, showing that the ultrathin film structure relaxes the requirement of phase matching in the SpFWM process. Then, the correlation function of the biphoton state is deduced, showing that the relaxation of phase match leads to the time-space factorability in the correlation function. It also leads to the spatiotemporal separability of the biphoton state, which is analyzed by the frequency purity when the spatial and polarization degrees of freedom are traced out. On the other hand, the spatial Schmidt numbers are calculated to show that high-dimensional transverse entanglement can be realized by this state. Finally, the feasibility of experimental observation of this biphoton state is evaluated numerically using different nonlinear ultrathin materials.

II. EXPRESSION OF BIPHOTON STATES GENERATED BY SpFWM IN ULTRATHIN FILM

The sketch of the biphoton state generation by SpFWM in a ultrathin film is shown in Fig. 1 (a). The film is made by a medium with high third order nonlinearity, which has a thickness of d . A linearly polarized pulsed pump light, which is shown by the red beam, illuminates the film at a

spot. The polarization direction of the pump beam is defined as x -axis and the surface of the ultrathin film is the x - y plane. Due to the ultrathin property of the nonlinear film and the polarization of pump beam, only the components $\chi_{xxxx}^{(3)}$ and $\chi_{yyyy}^{(3)}$ in the nonlinear susceptibility tensor are effective in SpFWM. The signal and idler photons generated by SpFWM would emit from the spot.

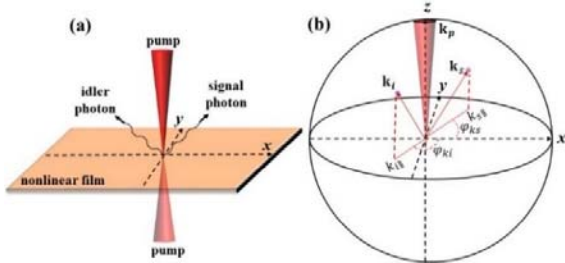


Fig.1 The illustrations of SpFWM in an ultrathin film. (a) The sketch shows the focused pump beam (red cone) and signal/idler photon emissions (wave lines). (b) The geometrical configuration in k -space.

To analyze the generated biphoton state, the Schrödinger equation of SpFWM process can be solved by perturbation method under low parametric gain [3, 9]. The solution provides the expression of the biphoton state $|\psi\rangle_{s-i}$

$$|\psi\rangle_{s-i} = \sum_{j_s=0,1} \sum_{j_i=0,1} \sum_{l_s=0,1} \sum_{l_i=0,1} \int d^6 \mathbf{S} \psi(\mathbf{S}, j_s, l_s, j_i, l_i) \times a_s^\dagger(\mathbf{S}_s, j_s, l_s) a_i^\dagger(\mathbf{S}_i, j_i, l_i) |0\rangle_s |0\rangle_i, \quad (1)$$

where $a_{s,i}^\dagger(\mathbf{S}_{s,i}, j_{s,i}, l_{s,i})$ ($a_{s,i}(\mathbf{S}_{s,i}, j_{s,i}, l_{s,i})$) is the creation (annihilation) operator for a mode with indices $\mathbf{S}_{s,i} = [\omega_{s,i}, \mathbf{k}_{s,i||}]$, $j_{s,i}=0,1$ and $l_{s,i}=0,1$. $\omega_{s,i}$ and $\mathbf{k}_{s,i||}$ are frequency and transverse wavevector (in plane component of the wave vector of the mode) of the signal/idler photons, respectively. $j_{s,i}=0$ ($j_{s,i}=1$) presents the modes propagating upwardly (downwardly) respect to the x - y plane. Here and henceforth, the “||” in the subscript means the variable is transverse. The electric fields of these modes are all linearly polarized, $l_{s,i}$ indicate two polarization directions. The modes with polarizations parallel with the x - y plane are indicated by $l_{s,i}=0$ and $l_{s,i}=1$ indicates that the modes polarized along the plane spanned by the propagating direction and z -axis. In the following discussion, the two polarization directions are represented as “TE” and “TM”, respectively. $\mathbf{k}_{s,i||}$ can be expressed by the spatial frequency $k_{s,i||} = |\mathbf{k}_{s,i||}|$ and angle $\varphi_{ks,i||}$, which are shown in Fig. 1 (b). The notation $|\cdot|$ means the magnitude of a vector or the modulus of a complex expression. The integral variable $\mathbf{S} = [\mathbf{S}_s, \mathbf{S}_i]$ in Eq. (1) is a six-dimensional vector. $\psi(\mathbf{S}, j_s, l_s, j_i, l_i)$ is the probability amplitude function for the signal and idler photons.

To simplify the calculation, we assume that the pump light is a series of Gaussian pulses with central frequency of ω_{p0} and temporal duration of τ_p . Its spatial distribution is Gaussian, and its waist is on the ultrathin film with a radius of r_p . The

peak power of the pump pulses is P_p . We also define two angular frequency detunings as $\Omega_{s,i} = \omega_{s,i} - \omega_{s,i0}$. Here, $\omega_{s,i0}$ is the central angular frequency of the signal or idler fields, which determined by the optical filters for the signal/idler photon collections and satisfied $\omega_{s0} + \omega_{i0} = 2\omega_{p0}$. In this case $\psi(\mathbf{S}, j_s, l_s, j_i, l_i)$ has an explicit expression (See the detailed derivation in Appendix A)

$$\psi(\Omega_s, \Omega_i, \mathbf{k}_{s||}, \mathbf{k}_{i||}, j_s, l_s, j_i, l_i) = \beta (\gamma P_p d_{eff}) (\pi r_p^2) (\sqrt{2} \pi \tau_p) \times G_\Omega(\Omega_s, \Omega_i) G_k(\mathbf{k}_{s||}, \mathbf{k}_{i||}) \Phi(\varphi_{ks}, \varphi_{ki}, l_s, l_i) \times \Theta(\Omega_s, k_{s||}, j_s, l_s) \Theta(\Omega_i, k_{i||}, j_i, l_i) U(\Omega_s, k_{s||}) U(\Omega_i, k_{i||}), \quad (2)$$

where γ is the third order nonlinear coefficient proportional to $\chi_{xxxx}^{(3)}$, but inverse proportional to r_p^2 . Here, β is a constant, and the explicit expressions of β and γ can be found in Appendix A. The constant d_{eff} is the effective nonlinear interaction length when the absorption of pump light, signal and idler photons in film are taken in to consideration. In Appendix F, the method to calculate d_{eff} for different types of material will be given. The terms $G_\Omega(\Omega_s, \Omega_i)$ and $G_k(\mathbf{k}_{s||}, \mathbf{k}_{i||})$ in Eq. (2) are

$$G_\Omega(\Omega_s, \Omega_i) = e^{-\tau_p^2 (\Omega_s + \Omega_i)^2 / 4}, \quad (3.1)$$

$$G_k(\mathbf{k}_{s||}, \mathbf{k}_{i||}) = e^{-r_p^2 |\mathbf{k}_{s||} + \mathbf{k}_{i||}|^2 / 4}, \quad (3.2)$$

and they originate from the energy and transverse momentum conservations in the SpFWM, respectively. The terms $\Phi(\varphi_{ks}, \varphi_{ki}, l_s, l_i)$ and $\Theta(\Omega_{s,i}, k_{s,i||}, j_{s,i}, l_{s,i})$ have forms of

$$\Phi(\varphi_{ks}, \varphi_{ki}, l_s, l_i) = \sum_{m=0,1} (\gamma_\chi)^m \cos(\varphi_{ks} + \frac{l_s - m}{2} \pi) \cos(\varphi_{ki} + \frac{l_i - m}{2} \pi), \quad (4.1)$$

$$\Theta(\Omega_{s,i}, k_{s,i||}, j_{s,i}, l_{s,i}) = \cos^{l_{s,i}} [\theta_{s,i}(\Omega_{s,i}, k_{s,i||}, j_{s,i})], \quad (4.2)$$

where $\theta_{s,i}(\Omega_{s,i}, k_{s,i||}, j_{s,i}) = (-1)^{j_{s,i}} \arcsin[k_{s,i||} / k_{s,i}(\Omega_{s,i})]$ is the angle between the wavevector of a mode and the z -axis, with $k_{s,i}(\Omega_{s,i})$ being the angular wavenumber at $\omega_{s,i}$. The parameter $\gamma_\chi = \chi_{yyyy}^{(3)} / \chi_{xxxx}^{(3)}$, indicating the anisotropy of the nonlinear susceptibility. The terms $U(\Omega_{s,i}, k_{s,i||}) = u[k_{s,i}(\Omega_{s,i}) - k_{s,i||}]$ in Eq. (2) are unit step functions. The angular wavenumbers $k_{s,i}(\Omega_{s,i})$ are related to the angular frequency detuning $\Omega_{s,i}$ via the dispersion relationship. In all the relevant numerical calculations in this paper, a linear dispersion relationship $k_{s,i} = (\omega_{s,i0} + \Omega_{s,i}) n_{s,i} / c$ is utilized, where $n_{s,i}$ is the refractive index of the ultrathin film.

Compared with expressions of biphoton states generated by SPDC in bulk crystals [9, 10], Eq. (2) has two differences. Firstly, there is no *sinc*-type factor in Eq. (2) since the phase mismatching effect is neglected in the integral along the longitudinal direction. Secondly, it has

two unit step functions, which are from that we truncate $\mathbf{k}_{s,i||}$ to only keep the spatial modes propagating along the longitudinal direction, and dropped all the evanescent modes along this direction. It is reasonable since usually the collection of signal/idler photons is in far field. By this way, the problem of divergence mentioned in Ref. [28] can be overcome.

For a specific signal (idler) mode with transverse wavevector $\mathbf{k}_{s||}$ ($\mathbf{k}_{i||}$), the joint spectral intensity [29] of the biphoton state shown in Eq. (2) can be explicitly expressed as $F(\Omega_s, \Omega_i) = e^{-r_p^2(\Omega_s + \Omega_i)^2/2}$, which extends homogeneously along the axis of $\Omega_s = -\Omega_i$ until that $k_s(\Omega_s) \geq k_{s||}$ and $k_i(\Omega_i) \geq k_{i||}$ are not satisfied. It is clearly different from the $F(\Omega_s, \Omega_i)$ of the biphoton states generated by SPDC in thick nonlinear media, in which the phase mismatching term makes $F(\Omega_s, \Omega_i)$ decay along the axis of $\Omega_s = -\Omega_i$ [29]. This difference means that the frequency bandwidth of the biphoton state generated by SpFWM in an ultrathin film could be much larger than that generated by SPDC in thick nonlinear crystals.

III. CORRELATION FUNCTION OF THE BIPHOTON STATE

The spatiotemporal structure of two photon correlation could be demonstrated by coincidence measurement of signal and idler photons under different time delay and spatial shift [16], which is in proportion to the modulus of correlation function of the biphoton state [15]. When the collection and detection processes of signal and idler photons are taken into consideration, the correlation function of the biphoton state described in Eq. (1) can be calculated by

$$C(t_s, t_i, \mathbf{r}_s, \mathbf{r}_i) = \langle 0 | \langle 0 | \hat{a}_s(t_s, \mathbf{r}_s) \hat{a}_i(t_i, \mathbf{r}_i) | \psi \rangle \\ = (2\pi)^{-3} \sum_{l_s=0,1} \sum_{l_i=0,1} \int d^6 \mathbf{S}' \psi(\mathbf{S}, 0, l_s, 0, l_i) F_{\Omega}(\Omega_s) F_{\Omega}(\Omega_i) \\ \times F_k(k_{s||}) F_k(k_{i||}) e^{-i(\Omega_s t_s + \Omega_i t_i)} e^{i(\mathbf{k}_{s||} \mathbf{r}_s + \mathbf{k}_{i||} \mathbf{r}_i)}, \quad (5)$$

where $\hat{a}_{s,i}(t_{s,i}, \mathbf{r}_{s,i})$ (see the explicit expressions of them in Appendix B) is the annihilation operators of signal/idler photons at time $t_{s,i}$ and positions $\mathbf{r}_{s,i} = r_{s,i} [\cos \varphi_{s,i}, \sin \varphi_{s,i}]$. In the collection configuration for deriving Eq. (5), only the photons propagating upwardly with respect to x - y plane are collected, and this results in the term $\psi(\mathbf{S}, j_s=0, l_s, j_i=0, l_i)$ inside the integral in Eq. (5). The terms $F_{\Omega}(\Omega_{s,i})$ and $F_k(k_{s,i||})$ are introduced to represent the filtering processes on the frequency and spatial frequency in the collection and detection after the biphoton generation, and in the calculation they have forms of

$$F_{\Omega}(\Omega_{s,i}) = e^{-(\Omega_{s,i}^2)/2\Omega_c^2}, \quad (6.1)$$

$$F_k(k_{s,i||}) = \begin{cases} 1 & \Upsilon_c k_{s,i||} < 1/2 \\ 0 & \text{others} \end{cases}. \quad (6.2)$$

In Eq. (6.1), the signal and idler channels have the same filtering bandwidth Ω_c . The filtering function shown in Eq. (6.2) corresponds to a lens which only collect the signal (idler) photons in modes with $k_{s,i||} < 1/2\Upsilon_c$.

When t_s and \mathbf{r}_s are set as the origins of temporal and spatial coordinate, an explicit expression of Eq. (5) can be obtained as

$$C(\Delta t, \Delta \mathbf{r}) \\ = C_c \sum_{l_s=0,1} \sum_{l_i=0,1} \int d\Omega_s \int d\Omega_i G_{\Omega}(\Omega_s, \Omega_i) F_{\Omega}(\Omega_s) F_{\Omega}(\Omega_i) e^{-i\Omega_i \Delta t} \\ \times \int k_{s||} dk_{s||} \int k_{i||} dk_{i||} g_k(k_{s||}, k_{i||}) I_1\left(\frac{r_p^2 k_{s||} k_{i||}}{2}\right) J(k_{i||}, \Delta r, \varphi_i) \\ \times \Theta(\Omega_s, k_{s||}, 0, l_s) \Theta(\Omega_i, k_{i||}, 0, l_i) U(\Omega_s, k_{s||}) U(\Omega_i, k_{i||}), \quad (7)$$

where Δt is the time delay and $\Delta \mathbf{r} = \Delta \mathbf{r} e^{i\varphi_i}$ is the spatial shift between the idler and signal photons. In Eq. (7), $g_k(k_{s||}, k_{i||}) = e^{-r_p^2(k_{s||}^2 + k_{i||}^2)/4}$ and $I_1(*)$ is the modified 1st-order Bessel function. The explicit expression of the constant C_c can be found in Appendix B. The expression of $J(k_{i||}, r_i, \varphi_i)$ is

$$J(k_{i||}, \Delta r, \varphi_i) = -\frac{1}{2}(1+r_{\chi})J_0(k_{i||}\Delta r) \cos\left[\frac{\pi}{2}(m_s - m_i)\right] \\ + \frac{1}{2}(1-r_{\chi})J_2(k_{i||}\Delta r) \cos\left[\frac{\pi}{2}(m_s + m_i) + 2\varphi_i\right], \quad (8)$$

where $J_0(*)$ and $J_2(*)$ are the 0th and 2nd-order Bessel functions, respectively. It is obvious that the correlation function in Eq. (7) is the sum of four terms which describe the spatial and temporal correlations between the photon pair with polarizations ‘TE/TE’, ‘TE/TM’, ‘TM/TE’ and ‘TM/TM’, respectively. In the following analysis, the four terms will be named as $C_{l_s l_i}(\Delta t, \Delta \mathbf{r})$ with $l_{s,i}=0,1$, and therefore $C(\Delta t, \Delta \mathbf{r}) = \sum_{l_s=0,1} \sum_{l_i=0,1} C_{l_s l_i}(\Delta t, \Delta \mathbf{r})$. All the four

terms have the form of cascaded two dimensional Fourier transformation and two dimensional Hankel transformation.

If we consider a special case that the pump is treated as a monochromatic plane wave. A simple form of $C_{l_s l_i}(\Delta t, \Delta \mathbf{r})$ is obtained as

$$C_{l_s l_i}(\Delta t, \Delta \mathbf{r}) = C_c \int d\Omega_s F_{\Omega}^2(\Omega_s) e^{i\Omega_s \Delta t} \int k_{s||} dk_{s||} \\ \times F_k^2(k_{s||}) J(k_{s||}, \Delta r, \varphi_i) \Theta(\Omega_s, k_{s||}, 0, l_s) \\ \times \Theta(\Omega_s, k_{s||}, 0, l_i) U(\Omega_s, k_{s||}). \quad (9)$$

This expression is the cascade of one dimensional Fourier transformation and one dimensional Hankel transformation. If $(\omega_{s0,i0} - \Omega_c)n_s/c \gg 1/\Upsilon_c$, i.e., the filtering bandwidths on the frequency and spatial frequency are not too large, $\Theta(\Omega_s, k_{s||}, 0, l_s)$, $\Theta(\Omega_s, k_{s||}, 0, l_i)$, and $U(\Omega_s, k_{s||})$ are always 1. In such case, Eq. (9) can be further simplified to

$$C_{l_s l_i}(\Delta t, \Delta \mathbf{r}) = C_c \int d\Omega_s F_{\Omega}^2(\Omega_s) e^{i\Omega_s \Delta t} \\ \times \int k_{s||} dk_{s||} F_k^2(k_{s||}) J(k_{s||}, \Delta r, \varphi_i). \quad (10)$$

This equation is similar with the correlation function of the biphoton state generated in SPDC in bulk nonlinear crystal

[30] pumped by plane wave, except two differences. Firstly, the kernel function in the Hankel transformation is different. Secondly, Eq. (10) can be factored to two parts only depending on Δt and $\Delta \mathbf{r}$, respectively, while the correlation function in Ref. [30] does not have this property. Since the Δt -dependent part is the same for all the four $C_{i,j}(\Delta t, \Delta \mathbf{r})$, the correlation function $C(\Delta t, \Delta \mathbf{r})$ of the biphoton state generated by SpFWM in ultrathin film can also be factored to temporal and spatial correlation functions. This means that the space and time in the biphoton state is factorable. Although this conclusion is obtained under the condition that $(\omega_{s0,i0} - \Omega_c)n_s / c \gg 1 / \Upsilon_c$, in Fig.2 we will show that it could be valid even when this condition is not satisfied well.

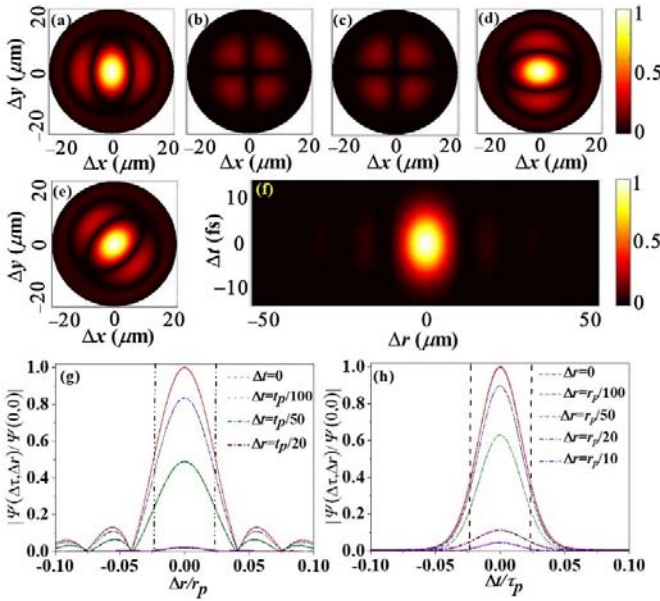


Fig. 2 The numerical calculations of the correlation function. (a)-(d) are $|C_{00}(0, \Delta \mathbf{r})|/|C_{00}(0,0)|$, $|C_{01}(0, \Delta \mathbf{r})|/|C_{00}(0,0)|$, $|C_{10}(0, \Delta \mathbf{r})|/|C_{00}(0,0)|$ and $|C_{11}(0, \Delta \mathbf{r})|/|C_{00}(0,0)|$ versus the spatial shifts $\Delta x = |\Delta \mathbf{r}| \cos \varphi_i$ and $\Delta y = |\Delta \mathbf{r}| \sin \varphi_i$. The vertical coordinates in (a)-(d) are the same, and the colorbar next to (d) is for all of (a)-(d). (e) The result of $|C(0, \Delta \mathbf{r})|$. (f) $|C(\Delta t, \Delta \mathbf{r})|/|C(0,0)|$ versus the Δr and Δt , when φ_i is set at $\pi/4$. The colorbar next to (f) is for both of (e) and (f). The calculations about (a-f) are based on Eq. (9). (g) $|C(\Delta t, \Delta \mathbf{r})|/|C(0,0)|$ versus Δr under different Δt . (h) $|C(\Delta t, \Delta \mathbf{r})|/|C(0,0)|$ versus Δt under different Δr . The calculations for (g) and (h) are based on Eq. (7). In (g) and (h), $\tau_p = 1\text{ps}$, $r_p = 10\mu\text{m}$, respectively. In all of the calculations, the central wavelength of the pump and idler fields are set as $\lambda_{p0} = 1530\text{nm}$ and $\lambda_{i0} = 1310\text{nm}$, respectively. Other parameters are $n_{i,s} = 2.6$, $r_x = 1/3$, $\Omega_c = 2\pi \times 50\text{THz}$ and $\Upsilon_c = 1\mu\text{m}$.

According to Eq. (9), we calculated all the four $C_{i,j}(0, \Delta \mathbf{r})$ under $\Omega_c = 2\pi \times 50\text{THz}$, $\Upsilon_c = 1\mu\text{m}$, and $r_x = 1/3$, i.e., $(\omega_{s0,i0} - \Omega_c)n_s / c \gg 1 / \Upsilon_c$ is not satisfied. The normalized results are shown in Figs. 2 (a) to (d). It is obvious that all the four terms are azimuthally anisotropic. This is different from the isotropic correlation function in Ref. [30], and the reason is

that the anisotropy of the nonlinear susceptibility is considered in our model. Moreover, $|C_{00}(0, \Delta r)|$ and $|C_{11}(0, \Delta r)|$ are much larger than $|C_{10}(0, \Delta r)|$ and $|C_{01}(0, \Delta r)|$, and therefore the former two are dominant in the calculation of $|C(0, \Delta r)|$. It is obvious that the orientations of $|C_{00}(0, \Delta r)|$ and $|C_{11}(0, \Delta r)|$ is along $\varphi_i = 0$ and $\varphi = 0$, respectively, and this makes $|C(0, \Delta \mathbf{r})|$ nearly orient along $\varphi = \pi/4$, which is calculated according to Eq. (9) and shown in the Fig. 2 (e). In Fig. 2 (f), $|C(\Delta t, \Delta \mathbf{r})|/|C(0,0)|$ versus Δt and Δr are shown with φ fixed at $\pi/4$ and $\Delta \mathbf{r} = \Delta r e^{i\pi/4}$. When Δt (Δr) is fixed at arbitrary position, $|C(\Delta t, \Delta \mathbf{r})|$ always shows Airy disk section (Gaussian) profile with variable of Δr (Δt), which corresponds to the profiles of the Hankel (Fourier) transformation of the filtering function in Eq. (6.1) (Eq. (6.2)). These results show that biphoton correlation of the state in Eq. (1) is factorable in temporal and spatial domains even under larger filtering bandwidths in frequency and spatial frequency. This property is much different from the biphoton state generated by SPDC in bulk nonlinear crystals. Their spatiotemporal structure of the biphoton correlation has nonfactorable X-geometry [30]. Such nonfactorability is determined by the requirement of phase match of SPDC in bulk crystals. On the other hand, for the biphoton state generated by SpFWM in ultrathin films, the factorability in the biphoton correlation revealed in Fig. 2 is due to the relaxation of the requirement of longitudinal phase match.

In the calculations for Fig. 2 (f), the pump beam is approximated by monochromatic plane wave. By numerically calculating the Eq. (7), we can study whether the biphoton correlation is factorable under Gaussian pump. The Monte Carlo method is employed to numerically compute the integrals in Eq. (7), when $\tau_p = 1\text{ps}$, $r_p = 10\mu\text{m}$ and other parameters are the same to these used in the calculation for Fig. 2 (f). The calculated results are shown in Figs. 2 (g) and (h). In Fig. 2 (g), the calculated normalized correlation function $|C(\Delta t, \Delta \mathbf{r})|/|C(0,0)|$ versus Δr is shown under different Δt . It can be seen that varying Δt does not change the Airy disk section profile of the calculated curves and its full width at half maxima (FWHM), which is the correlation length of the biphoton state. It only leads to the variation of magnitude of the curves. Figure 2 (h) shows the calculated $|C(\Delta t, \Delta \mathbf{r})|/|C(0,0)|$ versus Δt , when Δr is set at different values. It can be seen that all the curves under different Δr have Gaussian profile. Their widths indicate the correlation time of the biphoton state, which are almost unchanged under different Δr . Only the magnitudes of these curves decreases with increasing Δr . The two figures indicate that the biphoton correlation is still factorable in temporal and spatial domains even that Gaussian spatial distribution of the pump light is considered.

IV. SPATIOTEMPORAL SEPARABILITY OF THE

BIPHOTON STATE

As shown in Fig. 2, the correlation function of the biphoton generated in ultrathin film has factorable spatiotemporal structure. Since the correlation function is calculated based on the expression of the biphoton state, the temporal and spatial degrees of freedom in the biphoton state itself would be separable. The separability of a quantum state in two degrees of freedom can be evaluated by the purity of quantum state when one of the degrees of freedom is traced out [21]. To explore the spatio-temporal separability of the biphoton state shown in Eq. (1), we calculate the frequency purity $\text{Tr}(\rho_{\omega_s, \omega_i}^2)$ by tracing out the both of the spatial and polarization degrees of freedom. The result is (See the detailed derivation in Appendix C) are

$$\text{Tr}(\rho_{\omega_s, \omega_i}^2) = \frac{B}{N^2}, \quad (11)$$

where

$$\begin{aligned} N = & \frac{1}{4} \sum_{l_s=0,1} \sum_{l_i=0,1} \int_{-\infty}^{\infty} d\Omega_s \int_{-\infty}^{\infty} d\Omega_i \int k_{s\parallel} dk_{s\parallel} \int k_{i\parallel} dk_{i\parallel} \\ & \times G_{\Omega}^2(\Omega_s, \Omega_i) g_k^2(k_{s\parallel}, k_{i\parallel}) F_{\Omega}^2(\Omega_s) F_{\Omega}^2(\Omega_i) F_k^2(k_{s\parallel}) F_k^2(k_{i\parallel}) \\ & \times I(k_{s\parallel}, k_{i\parallel}, l_s, l_i) \Theta^2(\Omega_s, k_{s\parallel}, 0, l_s) \Theta^2(\Omega_i, k_{i\parallel}, 0, l_i) \\ & \times U(\Omega_s, k_{s\parallel}) U(\Omega_i, k_{i\parallel}), \end{aligned} \quad (12)$$

and

$$\begin{aligned} B = & \sum_{l_{s1}=0,1} \sum_{l_{i1}=0,1} \sum_{l_{s2}=0,1} \sum_{l_{i2}=0,1} \int_{-\infty}^{\infty} d\omega_{s1} \int_{-\infty}^{\infty} d\omega_{i1} \int_{-\infty}^{\infty} d\omega_{s2} \int_{-\infty}^{\infty} d\omega_{i2} \\ & \times \int k_{s1\parallel} dk_{s1\parallel} \int k_{s2\parallel} dk_{s2\parallel} \int k_{i1\parallel} dk_{i1\parallel} \int k_{i2\parallel} dk_{i2\parallel} \\ & \times \left[\prod_{m=1,2} G_{\Omega}^2(\Omega_{sm}, \Omega_{im}) g_k^2(k_{sm\parallel}, k_{im\parallel}) F_{\Omega}^2(\Omega_{sm}) F_{\Omega}^2(\Omega_{im}) \right. \\ & \times F_k^2(k_{sm\parallel}) F_k^2(k_{im\parallel}) I(k_{sm\parallel}, k_{im\parallel}, l_{sm}, l_{im}) \left. \right] \\ & \times \left[\prod_{\alpha=1,2} \prod_{\beta=1,2} \Theta^2(\Omega_{s\alpha}, k_{s\beta\parallel}, 0, l_{s\beta}) \right. \\ & \times \Theta^2(\Omega_{i\alpha}, k_{i\beta\parallel}, 0, l_{i\beta}) U(\Omega_{s\alpha}, k_{s\beta\parallel}) U(\Omega_{i\alpha}, k_{i\beta\parallel}) \left. \right]. \end{aligned} \quad (13)$$

In Eqs. (12) and (13), the term $I(k_{s\parallel}, k_{i\parallel}, l_s, l_i)$ is defined as

$$\begin{aligned} I(k_{s\parallel}, k_{i\parallel}, l_s, l_i) = & (1 + r_{\chi}^2) I_0(r_p^2 k_{s\parallel} k_{i\parallel}) \\ & + (1 + r_{\chi}^2) \cos[(l_s - l_i)\pi] I_2(r_p^2 k_{s\parallel} k_{i\parallel}). \end{aligned} \quad (14)$$

Compared with the denominator in Eq. (11), the numerator has eight additional terms, four cosine and four unit step functions in the integral. All the eight terms are smaller than 1 and this guarantees $\text{Tr}(\rho_{\omega_s, \omega_i}^2) \leq 1$ according to Eq. (11). When Ω_c is small and Υ_c is relatively large, i.e., the detection process is narrowband in both of the frequencies and spatial frequencies, all of the eight additional terms are nearly unit. In such case, the denominator and numerator in Eq. (10) is equal, leading to $\text{Tr}(\rho_{\omega_s, \omega_i}^2) = 1$. It shows that the biphoton state are separable in its temporal and spatial degrees of freedoms. This conclusion is consistent with the limit case shown in Ref. [21], where the two degrees of freedoms are separable in the biphoton state generated by SPDC in bulk crystal when the filtering bandwidth of the frequency is nearly 0 or that of the spatial frequency is very small.

When the bandwidths of the frequency and spatial frequency

filtering processes increases, Eq. (10) cannot be simplified in the way mentioned above. We calculate the evolution of the frequency purity with increasing Υ_c and under different Ω_c , numerically according to Eqs. (10), (11), and (12), and show the results in Fig. 3. The multi-dimensional integrals in Eq. (11) and (12) are implemented by the Monte Carlo methods. In the calculations, the rectangular filtering function in Eqs. (6.2) and (11) is replaced by $F_k(k_{s\parallel}) = e^{-\Upsilon_c^2 k_{s\parallel}^2 / 2}$, to make the comparison between our results and the results of similar calculation for biphoton state generated by SPDC in bulk crystal [21] reasonable, in which the filtering function of spatial frequency is Gaussian.

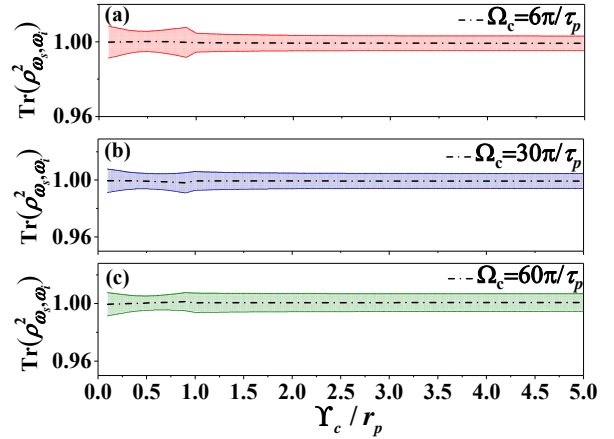


Fig. 3 The numerical calculations of the frequency purity $\text{Tr}(\rho_{\omega_s, \omega_i}^2)$. In (a), (b) and (c), the purity versus Υ_c is calculated when Ω_c are set at $6\pi/\tau_p$, $30\pi/\tau_p$, and $60\pi/\tau_p$, respectively. All the other parameters in the calculation for (a), (b) and (c) are the same to those used in Fig. (2). In each figure, the shadow band shows the results of 50 times of numerical computations involving Monte Carlo integrals for each case, the dashed dot line is their average.

Figure 3 (a) is the result under different Υ_c when the frequency filtering bandwidth is set 3THz. The shadow band shows the results of 50 times of numerical computations involving Monte Carlo integrals for each case, and the dashed dot curve is their average. It can be seen that the calculated purity $\text{Tr}(\rho_{\omega_s, \omega_i}^2)$ is always close to 1 under varying Υ_c . Figure 3 (b) and (c) show the results when the frequency filtering bandwidth increases to 30THz and 60 THz, respectively. It can be seen that the purity is still close to 1 with broader Ω_c . These results indicate that the temporal and spatial degrees of freedoms of the biphoton state studied here are separable, even under such large temporal and spatial filtering bandwidths. As a comparison, previous works of the analysis on biphoton states generated by SPDC in bulk crystals [11] shows that for the biphoton state generated in a crystal with a length of 1mm, the state purity would drop to near 0.2 when $\Omega_c/2\pi=4.7\text{THz}$ and $\Upsilon_c=100\mu\text{m}$. Hence, it is concluded that the biphoton states generated by SpFWM in ultrathin film are spatiotemporally separable even under large photon collection/detection frequency and spatial frequency bandwidths, thanks to the relaxation of the

requirement on longitudinal phase match. Since the separability between different degrees of freedom is important for the demonstration of hyper-entanglement, therefore ultrathin film is a type of promising material for realizing biphoton hyper-entanglement [21].

V. HIGH DIMENSIONAL TRANSVERSE ENTANGLEMENT IN BIPHOTON STATE

Above analysis shows that the requirement of longitude phase match relaxes in SpFWM in ultrathin films. On the other hand, the transverse phase match in this process still is required. It leads to the property of high dimensional transverse entanglement, which can be indicated by the spatial Schmidt number. Larger spatial Schmidt number means higher entanglement dimension [28]. The spatial Schmidt number can be obtained by Schmidt decomposition of the biphoton state under the bases of plane wave modes [28,31]. Here, we calculated the spatial Schmidt number to show the high dimensional transverse entanglement in the biphoton state generated by SpFWM in an ultrathin film.

Firstly, the spatial Schmidt number is obtained by $K_F = 1 / \text{Tr}[\rho^2(\mathbf{k}_{s\parallel}, \mathbf{k}_{i\parallel})]$, in which $\rho(\mathbf{k}_{s\parallel}, \mathbf{k}_{i\parallel})$ is the density matrix of the biphoton state in the subspace spanned by $\mathbf{k}_{s\parallel}$ and $\mathbf{k}_{i\parallel}$ [11]. Under the assumption that only the upwardly propagating photons with specific signal and idler frequencies are collected, the explicit expression of K_F can be deduced (see the detailed derivation in Appendix D) from the expression of the biphoton state in Eq. (2), and it has form of

$$K_F = \frac{N_K^2}{T}, \quad (15)$$

where

$$N_K = \sum_{l_s=0,1} \sum_{l_i=0,1} \int d\mathbf{k}_{s\parallel} \int d\mathbf{k}_{i\parallel} |\psi(\mathbf{k}_{s\parallel}, \mathbf{k}_{i\parallel}, l_s, l_i)|^2, \quad (16)$$

and

$$T = \sum_{l_{s1}=0,1} \sum_{l_{i1}=0,1} \sum_{l_{s2}=0,1} \sum_{l_{i2}=0,1} \int d\mathbf{k}_{s1\parallel} \int d\mathbf{k}_{s2\parallel} \int d\mathbf{k}_{i1\parallel} \int d\mathbf{k}_{i2\parallel} \\ \times \psi(\mathbf{k}_{s1\parallel}, \mathbf{k}_{i1\parallel}, l_{s1}, l_{i1}) \psi^*(\mathbf{k}_{s2\parallel}, \mathbf{k}_{i1\parallel}, l_{s1}, l_{i1}) \\ \times \psi(\mathbf{k}_{s2\parallel}, \mathbf{k}_{i2\parallel}, l_{s2}, l_{i2}) \psi^*(\mathbf{k}_{s4\parallel}, \mathbf{k}_{i2\parallel}, l_{s2}, l_{i2}). \quad (17)$$

The $\psi(\mathbf{k}_{s\parallel}, \mathbf{k}_{i\parallel}, l_s, l_i)$ in Eqs. (15) and (16) is the $\psi(\Omega_s, \Omega_i, \mathbf{k}_{s\parallel}, \mathbf{k}_{i\parallel}, j_s, l_s, j_i, l_i)$ in Eq. (3) with fixed Ω_s, Ω_i and $j_{s,i} = 1$. Though the implementation of the integrals about φ_{ks} and φ_{ki} in Eqs. (15) and (16) can give expressions (the Eqs. (D9-D18) in Appendix D) appropriate for calculating K_F numerically, they are too complex to give intuitionistic physical picture. To get this, we take two assumptions. First, only the photon pairs with “HH” polarizations are collected. Second, r_p is relatively large so that the term $G_{\mathbf{k}_{s\parallel}}(\mathbf{k}_{s\parallel}, \mathbf{k}_{i\parallel})$ in $\psi(\mathbf{k}_{s\parallel}, \mathbf{k}_{i\parallel}, l_s, l_i)$ can be approximated by $4\pi\delta(\mathbf{k}_{s\parallel} + \mathbf{k}_{i\parallel}) / r_p^2$. Under the two assumptions, we get an approximation of K_F as (See detailed derivation in Appendix D)

$$K_F = \frac{1}{8} \frac{\int d\mathbf{k}_{s\parallel} U(\Omega_s, k_{s\parallel}) U(\Omega_i, k_{s\parallel})}{\frac{2\pi}{r_p^2}}. \quad (18)$$

An approximated expression of the spatial Schmidt number of the biphoton state generated by SPDC in thick crystal can be obtained as (See detailed derivation in Appendix D)

$$K_S = \frac{3}{8} \frac{\int d\mathbf{k}_{s\parallel} \text{sinc}^2(\Delta k L) U(\Omega_s, k_{s\parallel}) U(\Omega_i, k_{s\parallel})}{\frac{2\pi}{r_p^2}}, \quad (19)$$

where Δk and L is the longitudinal phase mismatch in the SPDC and the thickness of the second order nonlinear crystal. The comparison between Eqs. (18) and (19) shows clear physics. In Eq. (18), the numerator has contributions of all the modes propagating along the longitudinal direction, while in Eq. (19), the numerator only has contributions of the modes satisfying the longitudinal phase matching condition. The denominators in Eqs. (18) and (19) are same and define the correlation volume [31]. Since the numerator in Eq. (19) is much smaller than that in Eq. (18), K_F is much larger than K_S under the same r_p . Therefore, the dimension of the transverse entanglement in the biphoton state generated by SpFWM in ultrathin films could be much higher than that of the state generated by SPDC in bulk crystal, due to the disappearance of the longitudinal phase mismatch. This conclusion is based on the two assumptions leading to Eq. (18), but in Fig. 4 it will be further verified by numerical calculations based on the Eq. (D9-D18) in Appendix D without any approximation.

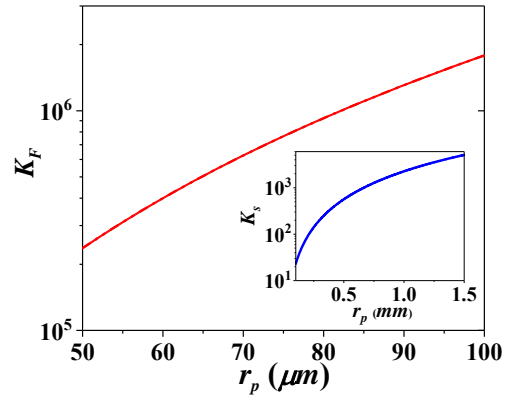


Fig. 4 The numerical calculations of the spatial Schmidt number K_F of the biphoton state generated by SpFWM in ultrathin film. The inset shows K_S for biphoton state generated by SPDC in a nonlinear crystal with a length of 1mm. In the calculations of SpFWM, $\lambda_p = 1530\text{nm}$, $\lambda_s = 1580\text{nm}$ and $n_{i,s} = 2.6$. In the calculations of SPDC, $\lambda_p = 405\text{nm}$ and $\lambda_s = \lambda_i = 810\text{nm}$, and $n_s = n_i = 1.7$.

According to Eq. (15-17), the spatial Schmidt number K_F is calculated numerically and the results are shown in Fig. 4. It can be seen that K_F increases with increasing r_p . According to Eq. (18), K_F can be considered as the ratio

between a certain volume and the correlation volume determined by r_p . Larger r_p gives lower correlation volume and leads to higher K_F . The spatial Schmidt number K_S versus r_p for the biphoton state generated by SPDC in a nonlinear crystal with a length of $L=1\text{mm}$ is also calculated according to the Eq. (23) in Ref. [11], and shown in Fig. 4 for comparison. The comparison between the two curves also show that even with smaller r_p , K_F could be much higher than K_S .

VI. DISCUSSION ON EXPERIMENTAL DEMONSTRATION

Coincidence photon counting measurement is the way to experimentally investigate the properties of biphoton states generated by SpFWM in ultrathin films. Since the nonlinear interaction length in an ultrathin film is very small, the key to demonstrate the biphoton state generation is whether sufficient coincidence photon counts can be recorded using proper materials and reasonable pump conditions. Several types of films, such as Au films and layered materials, have proven their high third-order nonlinearity [25, 32, 33]. In the following discussions, we will estimate the coincidence photon count rates of the photon pairs generated by SpFWM in some typical ultrathin films.

Consider that a pulsed pump light illuminates the ultrathin film in the vertical direction. It is a Gaussian beam with a Gaussian temporal pulse profile. Its waist locates on the film. The generated signal and idler photons are collected by a multi-mode collection system. Specifically, they are collected by lens with angular aperture of θ_c , pass the corresponding frequency filters with unified angular frequency bandwidth of Ω_c , and finally detected by two single photon detection devices with effective area of πr_c^2 . When θ_c and Ω_c are not too large, the coincidence photon count rate per pulse can be estimated by the following equation (see the detailed derivation in Appendix E)

$$n_c \approx \alpha_c \eta_s \eta_i (\gamma P_p d_{\text{eff}})^2 \Omega_c \tau_p \sin^2 \frac{\theta_c}{2} \left(\frac{r_c}{\lambda_{p0}} \right)^2 \times \left[\left(\frac{1+\gamma_z}{2} \right)^2 + \left(\frac{1-\gamma_z}{2} \right)^2 \right], \quad (20)$$

where $\alpha_c = n_p^2 \pi^2 / 9$, η_s (η_i) and λ_{p0} are the detection efficiency of the signal (idler) photons and the central wavelength of the pump light, respectively.

According to Eq. (20), the coincidence count rate n_c is calculated when graphene, Bi_2Se_3 and Au films are considered. In Fig. 5 (a), n_c are plotted with the increasing material thickness d . In the calculation, the pump pulse width τ_p and peak power P_p are 200fs and 80W, respectively. Graphene and Bi_2Se_3 are treated as layered materials in the calculations, and therefore their thicknesses increase discretely.

It is obvious in Fig.5 (a) that for the three ultrathin films, the coincidence count rate due to SpFWM are much higher. It can be seen that n_c for graphene and Bi_2Se_3 is much higher than that for Au films. It is partly due to the higher nonlinear refractive index of graphene and Bi_2Se_3 , and partly due to the stronger absorption in Au films. According to Eqs. (F2) and (F3) in Appendix F, d_{eff} will increase first and then

decreases when the thickness of Au film or the layers of graphene and Bi_2Se_3 increase. This results from the strong absorptions in the materials, and leads to the maximum in the curves of n_c in Fig.5 (a) for all of the three materials.

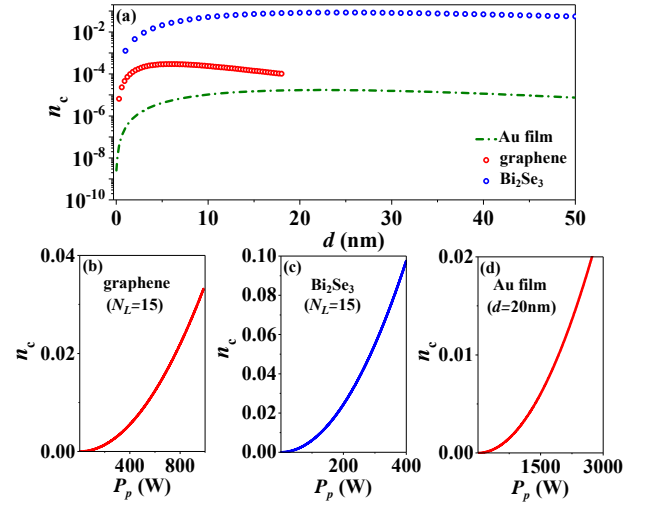


Fig. 5 The theoretical calculations of signal-idler coincidence photon count rate n_c in different nonlinear films and under different pump conditions. (a) n_c under increasing material thickness d for graphene (red circles), Bi_2Se_3 film (blue circles) and Au film (green dashed dot line), respectively. (b) to (d) show n_c versus P_p using the three materials, respectively. The vertical dotted lines in (b) and (d) for graphene and Au thin film indicate their damage threshold, respectively. In the calculation for (a), the pulse width and peak power of the pump light are 200fs and 80W, respectively. The pump and signal wavelengths used in calculations, the nonlinear susceptibilities or nonlinear refractive index of different materials, and linear and nonlinear losses of different materials are available in Table F1 the Appendix F.

The Fig. 5 (b), (c) and (d) show n_c under increasing P_p for different materials. Here, the layer numbers of both graphene and Bi_2Se_3 are $N_L=15$, and the thickness of Au film is 20nm. It can be seen that the coincidence count rate for graphene exceeds 0.01 per pulse when P_p is 500W. For Bi_2Se_3 film, n_c approximates 0.1 per pulse when P_p is 400W. For Au film, although the nonlinearity is lower than the former two materials, it can be compensated by higher P_p . It can be seen that $n_c > 0.01$ can be obtained under $P_p > 19.3\text{kW}$ in Fig.5 (d). In the calculations about Figs. 5 (a-d), r_p and τ_p are always kept at $5\mu\text{m}$ and 200fs, respectively. The damage thresholds of graphene and Au film are around $14\text{mJ}/\text{cm}^2$ [34] and $100\text{mJ}/\text{cm}^2$ [35], respectively, which correspond to $P_p = 55\text{kW}$ and $P_p = 393\text{kW}$, respectively, with r_p and τ_p mentioned above. In Ref. [33], even when the peak intensity of the incident laser pulses reaches $10.4\text{GW}/\text{cm}^2$, corresponding to $P_p = 8.16\text{kW}$ with $r_p = 5\mu\text{m}$, Bi_2Se_3 shows no damage. Therefore, the peak powers of pump light used in estimating n_c in Figs. 5 (a-d) are far away from the damage thresholds of the materials. These calculations indicate that the biphoton state generated by SpFWM in ultrathin films could be demonstrated by proper material selection and

reasonable pumping condition, with considerable coincidence count rates for applications on quantum optics and quantum information involving high-dimensional entanglement.

Under the pump power levels used in the calculation in Fig. 5 (b), (c) and (d), Kerr effect might become significant and its influence should be taken into consideration. Since the longitudinal phase mismatching term in the expression of the biphoton state disappears in ultra-thin materials, the change of the refractive index due to Kerr effect may influence the biphoton state only via the unit step functions presenting the truncation of the transverse wavevectors. However, in the numerical calculations of correlation functions in Fig. 2 and frequency purities in Fig. 3, as well as the evaluations of coincidence count in Fig. 5, the unit step function is always 1 within filtering bandwidths. Hence, the Kerr effect has little impact on the results shown in the three figures. Also, it can be calculated that the changes of the refractive index in Au film, graphene and Bi₂Se₃ are 0.017, 0.005 and 0.05 when the pump powers are set at 2kW, 500W and 400W, respectively, for the three materials. Substituting these refractive index changes into the calculations of Eq. (18), it can be seen that the corresponding changes of K_F are all smaller than 4%. Hence, the Kerr effect also has little impact on the results of Fig. 4.

In conclusion, we have theoretically investigated the biphoton state generated by SpFWM in ultrathin nonlinear films. The expression of the biphoton state is obtained by perturbation method under low parametric gain. Thanks to the ultrathin film structure, the requirement of longitudinal phase

match is relaxed, supporting very broad frequency bandwidth of the biphoton state. On the other hand, the spatial frequency in the expression is truncated to keep only the longitudinal propagating modes, by which the divergence problem mentioned in Ref. [28] can be overcome. Then, the spatial-temporal structure of the correlation function of the state is analyzed, showing that the space and time in the biphoton correlation are factorable due to the relaxation of the longitude phase match. By analyzing the state purity when the space and polarization degrees of freedom are traced out, the time-space factorability of the biphoton state is also demonstrated numerically. We also calculated the spatial Schmidt numbers of the state, indicating that high dimensional transverse entanglement could be realized by this way. Finally, the feasibility of experimental demonstration of this biphoton state generation is evaluated numerically using some typical nonlinear ultrathin materials, showing its potential on applications involving hyper-entanglement and high dimensional entanglement.

ACKNOWLEDGMENTS

This work was supported by the National Key R&D Program of China under Contract No. 2017YFA0303704, National Natural Science Foundation of China under Contract Nos. 61575102, 61875101, 91750206 and 61621064, Beijing Natural Science foundation under Contract No. Z180012, and Beijing Academy of Quantum Information Sciences under Contract No. Y18G26.

APPENDIX A: DERIVATION OF THE EXPRESSION OF THE BIPHOTON STATE

In the interaction, the pump is treated as classical electromagnetic waves. For simplicity, we assume the pump field has Gaussian-shape dependence on time t and spatial coordinates x and y in the transverse plane of the thin film. It is linearly polarized and the polarization is parallel to the x axis. Also, the paraxial approximation is used and we replace the a spherical wavefront by a plane wavefront with the value of the vector in z direction being k_{pz} . Under these assumptions, the electrical field intensity of the pump can be expressed as:

$$\begin{aligned} \mathbf{E}_p(t, x, y, z) &= \hat{\mathbf{x}}E_p^{(+)}(t, x, y, z) + \hat{\mathbf{x}}E_p^{(-)}(t, x, y, z) \\ &= \hat{\mathbf{x}}E_0 e^{-\frac{t^2}{2\tau_p^2}} e^{-\frac{(x^2+y^2)}{2r_p^2}} e^{i(k_{pz}z - \omega_p t)} + \hat{\mathbf{x}}E_0 e^{-\frac{t^2}{2\tau_p^2}} e^{-\frac{(x^2+y^2)}{2r_p^2}} e^{-i(k_{pz}z - \omega_p t)}, \end{aligned} \quad (A1)$$

where ω_p , τ_p and r_p are the central angular frequency, temporal duration and the transverse radius of the pump beam. Here, $\hat{\mathbf{x}}$ is the unit vector along x axis. After implementing the Fourier transformation for t , x and y , we express the electrical field in the domains of frequency and spatial frequencies as

$$\begin{aligned} \mathbf{E}_p(\omega_p, k_{px}, k_{py}, z) &= \hat{\mathbf{x}}E_p^{(+)}(\omega_p, k_{px}, k_{py}, z) + \hat{\mathbf{x}}E_p^{(-)}(\omega_p, k_{px}, k_{py}, z) \\ &= \hat{\mathbf{x}}E_0 \tau_p r_p^2 e^{-\frac{r_p^2(k_{px}^2 + k_{py}^2)}{2}} \left[e^{-\frac{\tau_p^2(\omega_p - \omega_{p0})^2}{2}} e^{ik_{pz}z} + e^{-\frac{\tau_p^2(\omega_p + \omega_{p0})^2}{2}} e^{-ik_{pz}z} \right], \end{aligned} \quad (A2)$$

where ω_p , k_{px} and k_{py} are frequency, the x and y component of the transverse wavevector of the pump field, respectively.

The quantized signal and idler fields generated in the SpFWM have expressions [36] of

$$\begin{aligned} \hat{\mathbf{E}}_s(t, x, y, z) &= \hat{\mathbf{E}}_s^{(+)}(t, x, y, z) + \hat{\mathbf{E}}_s^{(-)}(t, x, y, z) \\ &= (2\pi)^{-\frac{3}{2}} i \int d\omega_s \sqrt{\frac{\hbar\omega_s}{2c\epsilon_0}} \int dk_{sx} \int dk_{sy} \sum_{j_s, l_s} \sum_{l_s=0,1} \hat{\mathbf{e}}_{s, l_s} \hat{a}_s(\omega_s, k_{sx}, k_{sy}, j_s, l_s) e^{i(k_{sx}x + k_{sy}y)} e^{i[(-1)^j k_{sz}z - \omega_s t]} u[k_s(\omega_s) - k_{s||}] \\ &\quad - (2\pi)^{-\frac{3}{2}} i \int d\omega_s \sqrt{\frac{\hbar\omega_s}{2c\epsilon_0}} \int dk_{sx} \int dk_{sy} \sum_{j_s, l_s} \sum_{l_s=0,1} \hat{\mathbf{e}}_{s, l_s} \hat{a}_s^\dagger(\omega_s, k_{sx}, k_{sy}, j_s, l_s) e^{-i(k_{sx}x + k_{sy}y)} e^{-i[(-1)^j k_{sz}z - \omega_s t]} u[k_s(\omega_s) - k_{s||}], \end{aligned} \quad (A3)$$

$$\hat{\mathbf{E}}_i(t, x, y, z) = \hat{\mathbf{E}}_i^{(+)}(t, x, y, z) + \hat{\mathbf{E}}_i^{(-)}(t, x, y, z)$$

$$\begin{aligned}
&= (2\pi)^{-\frac{3}{2}} i \int d\omega_i \sqrt{\frac{\hbar\omega_i}{2c\epsilon_0}} \int dk_{ix} \int dk_{iy} \sum_{j_i=0,1} \sum_{l_i=0,1} \hat{\mathbf{e}}_{i,l_i} \hat{a}_i(\omega_i, k_{ix}, k_{iy}, j_i, l_i) e^{i(k_{ix}x + k_{iy}y)} e^{i[(-1)^{j_i} k_{iz}z - \omega_i t]} u[k_i(\omega_i) - k_{i\parallel}] \\
&- (2\pi)^{-\frac{3}{2}} i \int d\omega_i \sqrt{\frac{\hbar\omega_i}{2c\epsilon_0}} \int dk_{ix} \int dk_{iy} \sum_{j_i=0,1} \sum_{l_i=0,1} \hat{\mathbf{e}}_{i,l_i} \hat{a}_i^\dagger(\omega_i, k_{ix}, k_{iy}, j_i, l_i) e^{i(k_{ix}x + k_{iy}y)} e^{-i[(-1)^{j_i} k_{iz}z - \omega_i t]} u[k_i(\omega_i) - k_{i\parallel}], \quad (A4)
\end{aligned}$$

where ω_s (ω_i), k_{sx} (k_{ix}) and k_{sy} (k_{iy}) are the frequency, the x -component and y -component of the transverse wavevectors of the signal (idler) field, respectively. The meaning of $j_{s,i}$ and $l_{s,i}$ have been given in the paragraph below Eq. (1) in Sec. II. The four indices $\omega_{s,i}$, $k_{sx,ix}$, $k_{sy,iy}$ and $j_{s,i}$ can determine the wavevector of a mode uniquely. For instance, if a mode has indices ω_s , k_{sx} and k_{sy} , its wavevector can be represented as $(k_{sx}, k_{sy}, (-1)^{j_s} \sqrt{k_s^2 - k_{sx}^2 - k_{sy}^2})$ in the Cartesian coordinate for the upwardly and downwardly propagating modes, respectively, where k_s is the total angular wavenumber and depend on ω_s via the dispersion relationship $k_s(\omega_s)$. In the summation in Eq. (A3) and (A4), $l_{s,i}=0$ and 1 presents the “TE” and “TM” polarizations, respectively. The vector $\hat{\mathbf{e}}_{s,0}$ and $\hat{\mathbf{e}}_{s,1}$ ($\hat{\mathbf{e}}_{i,0}$ and $\hat{\mathbf{e}}_{i,1}$) are the unit vectors along the “TE” and “TM” polarization direction for signal (idler) photons. The operators of $\hat{a}_s(\omega_s, k_{sx}, k_{sy}, j_s, l_s)$ ($\hat{a}_i(\omega_i, k_{ix}, k_{iy}, j_i, l_i)$) and $\hat{a}_s^\dagger(\omega_s, k_{sx}, k_{sy}, j_s, l_s)$ ($\hat{a}_i^\dagger(\omega_i, k_{ix}, k_{iy}, j_i, l_i)$) are the annihilation and creation operators of the signal (idler) fields, respectively. It is notable that the dimensions of $\langle \hat{a}_{s,j,l}^\dagger(\omega_s, k_{sx}, k_{sy}) \hat{a}_{s,j,l}(\omega_s, k_{sx}, k_{sy}) \rangle$ ($\langle \hat{a}_{i,j,l}^\dagger(\omega_i, k_{ix}, k_{iy}) \hat{a}_{i,j,l}(\omega_i, k_{ix}, k_{iy}) \rangle$) is the photon number within unit volume in the space spanned by ω_s , k_{sx} and k_{sy} (ω_i , k_{ix} and k_{iy}). In Eq. (A3) and (A4), $u[k_s(\omega_s) - k_{s\parallel}]$ ($u[k_i(\omega_i) - k_{i\parallel}]$) is a unit step function, in which $k_{s\parallel} = \sqrt{k_{sx}^2 + k_{sy}^2}$ ($k_{i\parallel} = \sqrt{k_{ix}^2 + k_{iy}^2}$) is the total transverse angular wavenumber of the signal (idler) field. By the two unit step functions, only the modes propagating along the z axis are kept in the calculation.

We can use the polar coordinate variables $(k_{s\parallel}, \varphi_{ks})$ and $(k_{i\parallel}, \varphi_{ki})$ to replace the Cartesian variables (k_{sx}, k_{sy}) and (k_{ix}, k_{iy}) . The relationship between the variables are $k_{sx} = k_{s\parallel} \cos \varphi_{ks}$, $k_{ix} = k_{i\parallel} \cos \varphi_{ki}$, $k_{sy} = k_{s\parallel} \sin \varphi_{ks}$ and $k_{iy} = k_{i\parallel} \sin \varphi_{ki}$, as shown in Fig. 1 (b). Also, an angle $\theta_s(\omega_s, k_{s\parallel}, j_s)$ and $\theta_i(\omega_i, k_{i\parallel}, j_i)$ ($j=1,2$) is defined to characterize the angle between z axis and the wavevector of a mode, and they can be calculated by $\sin \theta_{s,i}(\omega_{s,i}, k_{s,i\parallel}, j_{s,i}) = (-1)^{j_{s,i}} k_{s,i\parallel} / k_{s,i}(\omega_{s,i})$. With these variables, we can get

$$\begin{aligned}
\hat{\mathbf{e}}_{s,0} &= -\sin \varphi_{ks} \hat{\mathbf{e}}_x + \cos \varphi_{ks} \hat{\mathbf{e}}_y \\
\hat{\mathbf{e}}_{i,0} &= -\sin \varphi_{ki} \hat{\mathbf{e}}_x + \cos \varphi_{ki} \hat{\mathbf{e}}_y \\
\hat{\mathbf{e}}_{s,1} &= \sin \theta_s \hat{\mathbf{e}}_z - \cos \theta_s \cos \varphi_{ks} \hat{\mathbf{e}}_x - \cos \theta_s \sin \varphi_{ks} \hat{\mathbf{e}}_y \\
\hat{\mathbf{e}}_{i,1} &= \sin \theta_i \hat{\mathbf{e}}_z - \cos \theta_i \cos \varphi_{ki} \hat{\mathbf{e}}_x - \cos \theta_i \sin \varphi_{ki} \hat{\mathbf{e}}_y \quad (A5)
\end{aligned}$$

The different polarization components of pump, signal and idler fields are coupled by different components in the nonlinear susceptibility tensor in the SpFWM. Considering that the polarizations of the pump fields are along x directions and assume that the materials has spatial inversion symmetry, only the tensor components $\chi_{yyyx}^{(3)}$ and $\chi_{xxxx}^{(3)}$ are effective in the SpFWM process. Then, the positive frequency part of the idler polarizations can be obtained as

$$\begin{aligned}
\hat{\mathbf{P}}_i^{(+)}(x, y, z, t) &= \chi^{(3)} \hat{\mathbf{x}} \hat{\mathbf{x}} [E_p^{(+)}(t, x, y, z)]^2 \sum_{j_s=1,2} \sum_{l_s=0,1} \hat{\mathbf{e}}_{s,l_s} \hat{E}_{s,j,l}^{(-)}(t, x, y, z) = -i(2\pi)^{-\frac{9}{2}} \int_{-\infty}^{\infty} d\omega_{p1} \int_{-\infty}^{\infty} d\omega_{p2} \int_{-\infty}^{\infty} d\omega_s \int_{-\infty}^{\infty} dk_{sx} \int_{-\infty}^{\infty} dk_{sy} \\
&\times \int_{-\infty}^{\infty} dk_{p1x} \int_{-\infty}^{\infty} dk_{p1y} \int_{-\infty}^{\infty} dk_{p2x} \int_{-\infty}^{\infty} dk_{p2y} [\hat{\mathbf{x}} \hat{P}_{ix}^{(+)}(x, y, z, t) + \hat{\mathbf{y}} \hat{P}_{iy}^{(+)}(x, y, z, t)], \quad (A6)
\end{aligned}$$

where

$$\begin{aligned}
\hat{P}_{ix}^{(+)}(x, y, z, t) &= -\chi_{xxxx} e^{i[(k_{p1x} + k_{p2x} - k_{sx})x + (k_{p1y} + k_{p2y} - k_{sy})y - (\omega_{p1} + \omega_{p2} - \omega_s)t]} E_p^{(+)}(\omega_{p1}, k_{p1x}, k_{p1y}, z) E_p^{(+)}(\omega_{p2}, k_{p2x}, k_{p2y}, z) \\
&\times \sum_{j_s=0,1} [\sin \varphi_{ks} \hat{a}_s^\dagger(\omega_s, k_{sx}, k_{sy}, j_s, 0) + \cos \theta_{ks} \cos \varphi_{ks} \hat{a}_{s,j,p}^\dagger(\omega_s, k_{sx}, k_{sy}, j_s, 1)] e^{i[k_{p1z} + k_{p2z} - (-1)^{j_s} k_{sz}]z}, \quad (A7)
\end{aligned}$$

and

$$\begin{aligned}
\hat{P}_{iy}^{(+)}(x, y, z, t) &= \chi_{yyyx} e^{i[(k_{sx} - k_{p1x} - k_{p2x})x + (k_{sy} - k_{p1y} - k_{p2y})y - (\omega_s - \omega_{p1} - \omega_{p2})t]} E_p^{(+)}(\omega_{p1}, k_{p1x}, k_{p1y}, z) E_p^{(+)}(\omega_{p2}, k_{p2x}, k_{p2y}, z) \\
&\times \sum_{j_s=1,2} [\cos \varphi_{ks} \hat{a}_s^\dagger(\omega_s, k_{sx}, k_{sy}, j_s, 0) - \cos \theta_{ks} \sin \varphi_{ks} \hat{a}_{s,j,p}^\dagger(\omega_s, k_{sx}, k_{sy}, j_s, 1)] e^{i[k_{p1z} + k_{p2z} - (-1)^{j_s} k_{sz}]z}, \quad (A8)
\end{aligned}$$

Then, the interaction Hamiltonian for the FWM parametric process takes the form of

$$\hat{H}_I = \varepsilon_0 \int_{-L_x/2}^{L_x/2} dx \int_{-L_y/2}^{L_y/2} dy \int_{-d/2}^{d/2} dz [\hat{\mathbf{P}}_i^{(+)}(x, y, z, t) * \hat{\mathbf{E}}_i^{(-)}(t, x, y, z) + \text{H.c.}], \quad (\text{A9})$$

where “*” presents the dot product. In Eq. (A8), L_x (L_y) are the size of the film along x (y) direction. Substituting Eqs. (A3), (A4) and (A5) into (A8) and implementing the integrals with variables x , y and z , we can get the explicit expression of \hat{H}_I as

$$\begin{aligned} \hat{H}_I = & -\hbar \chi_{xxxx}^{(3)} \frac{(\tau_p r_p^2)^2}{2c} (2\pi)^{-6} E_0^2 \sum_{j_s=0,1} \sum_{j_i=0,1} \sum_{l_s=0,1} \sum_{l_i=0,1} \int d\omega_s \int d\omega_i \int d\omega_{p1} \int d\omega_{p2} \sqrt{\omega_s \omega_i} e^{-i\Delta\omega t} e^{-\frac{\tau_p^2[(\omega_{p1}-\omega_{p0})^2+(\omega_{p2}-\omega_{p0})^2]}{2}} \\ & \times \int dk_{p1x} \int dk_{p1y} \int dk_{p2x} \int dk_{p2y} \int dk_{sx} \int dk_{sy} \int dk_{ix} \int dk_{iy} L_x L_y d \text{sinc}(\Delta k_x L_x / 2) \text{sinc}(\Delta k_y L_y / 2) \\ & \times \text{sinc}\{[k_{p1}+k_{p2}-(-1)^{j_s} k_{sz}-(-1)^{j_i} k_{iz}]d/2\} e^{-\frac{r_p^2[(k_{p1x}^2+k_{p1y}^2)+(k_{p2x}^2+k_{p2y}^2)]}{2}} \cos^{l_s}[\theta_s(\omega_s, k_{s||}, j_s)] \cos^{l_i}[\theta_i(\omega_i, k_{i||}, j_i)] \\ & \times \sum_{m=0,1} (r_\chi)^m \cos(\varphi_{ks} + \frac{l_s-m}{2}\pi) \cos(\varphi_{ki} + \frac{l_i-m}{2}\pi) \hat{a}_s^\dagger(\omega_s, k_{sx}, k_{sy}, j_s, l_s) \hat{a}_i^\dagger(\omega_i, k_{ix}, k_{iy}, j_i, l_i), \end{aligned} \quad (\text{A10})$$

where $\Delta\omega = \omega_{p1} + \omega_{p2} - \omega_s - \omega_i$, $\Delta k_x = k_{p1x} + k_{p2x} - k_{sx} - k_{ix}$ and $\Delta k_y = k_{p1y} + k_{p2y} - k_{sy} - k_{iy}$. To simplify the calculation, the dependence of $\chi_{xxxx}^{(3)}$ on the angular frequencies of pump, signal and idler fields are neglected in the derivation of Eq. (A9). Similar with the treatment for SPDC [36], we consider that the size of the ultrathin film in the x - y plane is much larger than the transverse size of pump beam, and the terms $L_x \text{sinc}(\Delta k_x L_x / 2)$ and $L_y \text{sinc}(\Delta k_y L_y / 2)$ can be replaced by $2\pi\delta(\Delta k_x)$ and $2\pi\delta(\Delta k_y)$. Also, since the film is ultrathin along z axis, the term $\text{sinc}\{[k_{p1}+k_{p2}-(-1)^{j_s} k_{sz}-(-1)^{j_i} k_{iz}]d/2\}$ can be approximated by 1, i.e., the longitudinal phase mismatch can be neglected. Under the two approximations, Eq. (A9) can be simplified as

$$\begin{aligned} \hat{H}_I = & -[(2\pi)^{-3} n_{p0} / 6] \gamma P_p d \tau_p^2 r_p^2 \sum_{j_s=0,1} \sum_{j_i=0,1} \sum_{l_s=0,1} \sum_{l_i=0,1} \int d\omega_s \int d\omega_i \int d\omega_{p1} \int d\omega_{p2} \frac{\sqrt{\omega_s \omega_i}}{c k_{p0}} e^{-\frac{\tau_p^2[(\omega_{p1}-\omega_{p0})^2+(\omega_{p2}-\omega_{p0})^2]}{2}} \\ & \times \int dk_{sx} \int dk_{sy} \int dk_{ix} \int dk_{iy} e^{-\frac{r_p^2[(k_{sx}-k_{ix})^2+(k_{sy}-k_{iy})^2]}{4}} \cos^{l_s}[\theta_s(\omega_s, k_{s||}, j_s)] \cos^{l_i}[\theta_i(\omega_i, k_{i||}, j_i)] \\ & \times \sum_{m=0,1} (r_\chi)^m \cos(\varphi_{ks} + \frac{l_s-m}{2}\pi) \cos(\varphi_{ki} + \frac{l_i-m}{2}\pi) \\ & \times \hat{a}_s^\dagger(\omega_s, k_{sx}, k_{sy}, j_s, l_s) \hat{a}_i^\dagger(\omega_i, k_{ix}, k_{iy}, j_i, l_i) \end{aligned} \quad (\text{A11})$$

where $\gamma = n_2 k_{p0} / (\pi r_p^2)$ with $k_{p0} = \omega_{p0} / c$ is the nonlinear coefficient in the SpFWM, and $P_p = 2(\pi r^2) n_{p0} \varepsilon_0 c E_0^2$ is the peak power of the pump pulses. Here, n_{p0} is the linear refractive index of the film at the central frequency of the pulsed pump light. In the introduction of P_p , E_0 is assumed to be real to simplify the calculations. A ratio $r_\chi = \chi_{yyxx}^{(3)} / \chi_{xxxx}^{(3)}$ is defined to indicate the anisotropy of the nonlinear susceptibility in the ultrathin film.

The initial states of the signal and idler fields are vacuum states and they evolves according to Schrödinger equation. For SpFWM, a perturbative solution of this equation is $|\psi\rangle_{s-i} \approx -(i/\hbar) \int_{-\infty}^{\infty} dt \hat{H}_I |0\rangle_s |0\rangle_i$ [9]. Substituting Eq. (A10) into this solution, we can get

$$\begin{aligned} |\psi\rangle_{s-i} \approx & \beta \gamma P_p d (\pi r_p^2) (\sqrt{\pi} \tau_p) \sum_{j_s=0,1} \sum_{j_i=0,1} \sum_{l_s=0,1} \sum_{l_i=0,1} \int d\omega_s \int d\omega_i e^{-\frac{\tau_p^2(\omega_s+\omega_i-2\omega_{p0})^2}{4}} \\ & \times \int dk_{sx} \int dk_{sy} \int dk_{ix} \int dk_{iy} e^{-\frac{r_p^2[(k_{sx}-k_{ix})^2+(k_{sy}-k_{iy})^2]}{4}} \cos^{l_s}[\theta_s(\omega_s, k_{s||}, j_s)] \cos^{l_i}[\theta_i(\omega_i, k_{i||}, j_i)] \\ & \times \sum_{m=0,1} (r_\chi)^m \cos(\varphi_{ks} + \frac{l_s-m}{2}\pi) \cos(\varphi_{ki} + \frac{l_i-m}{2}\pi) \hat{a}_s^\dagger(\omega_s, k_{sx}, k_{sy}, j_s, l_s) \hat{a}_i^\dagger(\omega_i, k_{ix}, k_{iy}, j_i, l_i) |0\rangle_s |0\rangle_i. \end{aligned} \quad (\text{A12})$$

where the parameter $\beta = i(2\pi)^{-3} n_{p0} / 3$. In the derivation of Eq. (A11), $|\omega_{s,i} - \omega_{p0}| \ll \omega_{p0}$ is assumed. The Eq. (A11) can be written in a compact form as

$$|\psi\rangle = \sum_{j_s=0,1} \sum_{j_i=0,1} \sum_{l_s=0,1} \sum_{l_i=0,1} \int d^6 \mathbf{S} \psi(\mathbf{S}, j_s, l_s, j_i, l_i) a_s^\dagger(\mathbf{S}_s, j_s, l_s) a_i^\dagger(\mathbf{S}_i, j_i, l_i) |0\rangle_s |0\rangle_i, \quad (\text{A13})$$

which is the Eq. (1) in Sec. II. The meanings of $\mathbf{S}_{s,i}$ and $\mathbf{k}_{s||,i||} = [k_{sx,ix}, k_{sy,iy}]$ can be found in the explanation of Eq. (1)

in Sec. II. $\psi(\mathbf{S}, j_s, l_s, j_i, l_i)$ is the biphoton probability amplitude function and its expression is shown in Eq. (2) in Sec. II.

APPENDIX B: CALCULATION OF CORRELATION FUNCTION

In the case that only the photons propagating upwardly with respect to x - y plane are collected, two spatiotemporally varying annihilation operators can be constructed as

$$\hat{a}_s(t_s, \mathbf{r}_s) = (2\pi)^{-3/2} \sum_{j_s=0,1} \sum_{l_s=0,1} \int d\Omega_s \int d^2\mathbf{k}_{s\parallel} \hat{a}_s(\Omega_s, \mathbf{k}_{s\parallel}, 0, l_s) F_\Omega(\Omega_s) F_k(k_{s\parallel}) e^{i(\mathbf{k}_{s\parallel} \cdot \mathbf{r}_s - \Omega_s t_s)}, \quad (\text{B1})$$

$$\hat{a}_i(t_i, \mathbf{r}_i) = (2\pi)^{-3/2} \sum_{j_i=0,1} \sum_{l_i=0,1} \int d\Omega_i \int d^2\mathbf{k}_{i\parallel} \hat{a}_i(\Omega_i, \mathbf{k}_{i\parallel}, 0, l_i) F_\Omega(\Omega_i) F_k(k_{i\parallel}) e^{i(\mathbf{k}_{i\parallel} \cdot \mathbf{r}_i - \Omega_i t_i)}, \quad (\text{B2})$$

where $F_\Omega(\Omega_{s,i})$ and $F_k(k_{s\parallel,i\parallel})$ are the frequency and spatial frequency filtering functions in the collection and detection of signal and idler photons. The filtering functions in our calculations are shown in the Eqs. (6.1) and (6.2) in Sec. III.

The correlation function can be calculated by [30]

$$C(t_s, \mathbf{r}_s, t_i, \mathbf{r}_i) = \langle 0 | \langle 0 | \hat{a}_s(t_s, \mathbf{r}_s) \hat{a}_i(t_i, \mathbf{r}_i) | \psi \rangle_{s-i}. \quad (\text{B3})$$

After substituting Eqs. (A12), (B1) and (B2) into (B3), and utilizing the commutation relationships

$$[\hat{a}_s(\Omega'_s, \mathbf{k}'_{s\parallel}, j'_s, l'_s), \hat{a}_i^\dagger(\Omega_i, \mathbf{k}_{i\parallel}, j_i, l_i)] = \delta(\Omega'_s - \Omega_i) \delta(\mathbf{k}'_{s\parallel} - \mathbf{k}_{i\parallel}) \delta_{j'_s j_i} \delta_{l'_s l_i}, \quad (\text{B4})$$

$$[\hat{a}_i(\Omega'_i, \mathbf{k}'_{i\parallel}, j'_i, l'_i), \hat{a}_s^\dagger(\Omega_s, \mathbf{k}_{s\parallel}, j_s, l_s)] = \delta(\Omega'_i - \Omega_s) \delta(\mathbf{k}'_{i\parallel} - \mathbf{k}_{s\parallel}) \delta_{j'_i j_s} \delta_{l'_i l_s}, \quad (\text{B5})$$

$$[\hat{a}_s(\Omega'_s, \mathbf{k}'_{s\parallel}, j'_s, l'_s), \hat{a}_i^\dagger(\Omega_i, \mathbf{k}_{i\parallel}, j_i, l_i)] = [\hat{a}_i(\Omega'_i, \mathbf{k}'_{i\parallel}, j'_i, l'_i), \hat{a}_s^\dagger(\Omega_s, \mathbf{k}_{s\parallel}, j_s, l_s)] = 0, \quad (\text{B6})$$

we get the expression of $C(t_s, \mathbf{r}_s, t_i, \mathbf{r}_i)$ as

$$\begin{aligned} C(t_s, t_i, \mathbf{r}_s, \mathbf{r}_i) &= \langle 0 | \langle 0 | \hat{a}_s(t_s, \mathbf{r}_s) \hat{a}_i(t_i, \mathbf{r}_i) | \psi \rangle \\ &= (2\pi)^{-3} \sum_{l_s=0,1} \sum_{l_i=0,1} \int d^6\mathbf{S} \psi(\mathbf{S}, 0, l_s, 0, l_i) F_\Omega(\Omega_s) F_\Omega(\Omega_i) F_k(k_{s\parallel}) F_k(k_{i\parallel}) e^{-i(\Omega_s t_s + \Omega_i t_i)} e^{i(\mathbf{k}_{s\parallel} \cdot \mathbf{r}_s + \mathbf{k}_{i\parallel} \cdot \mathbf{r}_i)}. \end{aligned} \quad (\text{B7})$$

After substituting Eq. (2) into Eq. (B7), we can get

$$\begin{aligned} C(t_s, t_i, \mathbf{r}_s, \mathbf{r}_i) &= C_c \sum_{l_s=0,1} \sum_{l_i=0,1} \int d\Omega_s \int d\Omega_i \int dk_{s\parallel} \int dk_{i\parallel} \int d\varphi_{ks} \int d\varphi_{ki} G_\Omega(\Omega_s, \Omega_i) G_k(\mathbf{k}_{s\parallel}, \mathbf{k}_{i\parallel}) \Phi(\varphi_{ks}, \varphi_{ki}, l_s, l_i) \\ &\quad \times \Theta(\Omega_s, k_{s\parallel}, 0, l_s) \Theta(\Omega_i, k_{i\parallel}, 0, l_i) U(\Omega_s, k_{s\parallel}) U(\Omega_i, k_{i\parallel}) F_\Omega(\Omega_s) F_\Omega(\Omega_i) F_k(k_{s\parallel}) F_k(k_{i\parallel}) e^{-i(\Omega_s t_s + \Omega_i t_i)} e^{i(\mathbf{k}_{s\parallel} \cdot \mathbf{r}_s + \mathbf{k}_{i\parallel} \cdot \mathbf{r}_i)}. \end{aligned} \quad (\text{B8})$$

where $C_c = (2\pi)^{-3} \beta \gamma P_p d_{\text{eff}} (\pi r_p^2) (\sqrt{\pi} \tau_p)$.

Considering the following equations

$$\mathbf{k}_{s\parallel} \cdot \mathbf{r}_s = k_{s\parallel} r_s \cos \varphi_s \cos \varphi_{ks} + k_{s\parallel} r_s \sin \varphi_s \sin \varphi_{ks} = k_{s\parallel} r_s \cos(\varphi_{ks} - \varphi_s), \quad (\text{B9})$$

$$\mathbf{k}_{i\parallel} \cdot \mathbf{r}_i = k_{i\parallel} r_i \cos \varphi_i \cos \varphi_{ki} + k_{i\parallel} r_i \sin \varphi_i \sin \varphi_{ki} = k_{i\parallel} r_i \cos(\varphi_{ki} - \varphi_i), \quad (\text{B10})$$

$$e^{ik_{s\parallel} r_s \cos(\varphi_{ks} - \varphi_s)} = \sum_{n=-\infty}^{\infty} i^n J_n(k_{s\parallel} r_s) e^{in(\varphi_s - \varphi_{ks})}, \quad (\text{B11})$$

$$e^{\frac{r_p^2 k_{s\parallel} k_{i\parallel}}{2} \cos(\varphi_{ks} - \varphi_{ki})} = \sum_{n=-\infty}^{\infty} (-1)^n I_n\left(\frac{r_p^2 k_{s\parallel} k_{i\parallel}}{2}\right) e^{in(\varphi_{ks} - \varphi_{ki})}, \quad (\text{B12})$$

we can finish the integrals about φ_{ks} and φ_{ki} in Eq. (B8) and get

$$\begin{aligned} C(\Delta t, \Delta r) &= C_c \sum_{l_s=0,1} \sum_{l_i=0,1} \int d\omega_s \int d\omega_i G_\Omega(\Omega_s, \Omega_i) F_\Omega(\Omega_s) F_\Omega(\Omega_i) e^{-i(\Omega_i t_i + \Omega_s t_s)} \\ &\quad \times \int k_{s\parallel} dk_{s\parallel} \int k_{i\parallel} dk_{i\parallel} g_k(k_{s\parallel}, k_{i\parallel}) J(k_{i\parallel}, \Delta r, \varphi_i) \\ &\quad \times \Theta(\Omega_s, k_{s\parallel}, 0, l_s) \Theta(\Omega_i, k_{i\parallel}, 0, l_i) U(\Omega_s, k_{s\parallel}) U(\Omega_i, k_{i\parallel}), \end{aligned} \quad (\text{B13})$$

where $g_k(k_{s\parallel}, k_{i\parallel}) = e^{-r_p^2(k_{s\parallel}^2 + k_{i\parallel}^2)/4}$. The expression of $J(k_{i\parallel}, r_i, \varphi_i)$ is

$$\begin{aligned} J(k_{i\parallel}, r_i, \varphi_i) &= \frac{1}{4} \sum_{n=-\infty}^{\infty} I_n\left(\frac{r_p^2 k_{s\parallel} k_{i\parallel}}{2}\right) \{J_{n+1}(k_{s\parallel} r_s) e^{i(n+1)\varphi_s} [(1 - r_\chi) J_{n-1}(k_{i\parallel} r_i) e^{-i(n-1)\varphi_i} e^{i(\frac{l_s + l_i}{2}\pi)} \\ &\quad - (1 + r_\chi) J_{n+1}(k_{i\parallel} r_i) e^{-i(n+1)\varphi_i} e^{i(\frac{l_s - l_i}{2}\pi)}] + J_{n-1}(k_{s\parallel} r_s) e^{i(n-1)\varphi_s} [(1 - r_\chi) J_{n+1}(k_{i\parallel} r_i) e^{-i(n+1)\varphi_i} e^{-i(\frac{l_s + l_i}{2}\pi)} \\ &\quad + (1 + r_\chi) J_{n-1}(k_{i\parallel} r_i) e^{-i(n-1)\varphi_i} e^{-i(\frac{l_s - l_i}{2}\pi)}]\} \end{aligned}$$

$$-(1+r_\chi)J_{n-1}(k_{i\parallel}r_i)e^{-i(n-1)\varphi_i}e^{-i\frac{l_s-l_i}{2}\pi}\}, \quad (\text{B14})$$

where $I_n(*)$, $J_{n+1}(*)$, and $J_{n-1}(*)$ are the n^{th} -order modified Bessel function, $(n+1)^{\text{th}}$ -order Bessel function, and $(n-1)^{\text{th}}$ -order Bessel function, respectively.

When \mathbf{r}_s is set at origin, i.e., $r_s = 0$, Eq. (14) is simplified to

$$J(k_{i\parallel}, r_i, \varphi_i) = \frac{1}{2} \{ (1+r_\chi)J_0(k_{i\parallel}r_i) \cos[\frac{\pi}{2}(l_s-l_i)] - (1-r_\chi)J_2(k_{i\parallel}r_i) \cos[\frac{\pi}{2}(l_s+l_i)+2\varphi_i] \}. \quad (\text{B15})$$

Equations (B13) and (B15) are the Eqs. (7) and (8) in Sec. III, respectively.

APPENDIX C: CALCULATION OF PURITY OF REDUCED DENSITY MATRIX

With the collection and detection configuration in the derivation of Eq. (5), we can get an effective biphoton probability amplitude function as [21]

$$\psi_e(\Omega_s, \Omega_i, \mathbf{k}_{s\parallel}, \mathbf{k}_{i\parallel}, l_s, l_i) = \psi(\Omega_s, \Omega_i, \mathbf{k}_{s\parallel}, \mathbf{k}_{i\parallel}, 0, l_s, 0, l_i) F_\Omega(\Omega_s) F_\Omega(\Omega_i) F_k(\mathbf{k}_{s\parallel}) F_k(\mathbf{k}_{i\parallel}), \quad (\text{C1})$$

Then an effective biphoton state can be written as

$$|\psi\rangle_e = \sum_{l_s=0,1} \sum_{l_i=0,1} \int d\Omega_s \int d\Omega_i \int d\mathbf{k}_{s\parallel} \int d\mathbf{k}_{i\parallel} \psi_e(\Omega_s, \Omega_i, \mathbf{k}_{s\parallel}, \mathbf{k}_{i\parallel}, l_s, l_i) a_s^\dagger(\Omega_s, \mathbf{k}_{s\parallel}, l_s) a_i^\dagger(\Omega_i, \mathbf{k}_{i\parallel}, l_i) |0\rangle_s |0\rangle_i, \quad (\text{C2})$$

To get its density matrix, this effective biphoton state should be normalized [11]. The normalized constant $|N_a|$ would be obtained by

$$|N_a|^2 \left[\sum_{l_s=0,1} \sum_{l_i=0,1} \int d\Omega_s \int d\Omega_i \int d\mathbf{k}_{s\parallel} \int d\mathbf{k}_{i\parallel} |\psi_e(\Omega_s, \Omega_i, \mathbf{k}_{s\parallel}, \mathbf{k}_{i\parallel}, l_s, l_i)|^2 \right] = 1. \quad (\text{C3})$$

The part within the bracket in Eq. (C3) can be expanded into

$$\begin{aligned} & \sum_{l_s=0,1} \sum_{l_i=0,1} \int d\Omega_s \int d\Omega_i \int d\mathbf{k}_{s\parallel} \int d\mathbf{k}_{i\parallel} |\psi_e(\Omega_s, \Omega_i, \mathbf{k}_{s\parallel}, \mathbf{k}_{i\parallel}, l_s, l_i)|^2 \\ &= C_0^2 \sum_{l_s=0,1} \sum_{l_i=0,1} \int d\Omega_s \int d\Omega_i \int dk_{s\parallel} \int dk_{i\parallel} \int d\varphi_{ks} \int d\varphi_{ki} G_\Omega^2(\Omega_s, \Omega_i) e^{\frac{r_p^2[k_{s\parallel}^2+k_{i\parallel}^2+2k_{s\parallel}k_{i\parallel}\cos(\varphi_{ks}-\varphi_{ki})]}{2}} \\ & \quad \times [r_\chi \sin(\varphi_{ks} + \frac{l_s\pi}{2}) \sin(\varphi_{ki} + \frac{l_i\pi}{2}) + \cos(\varphi_{ks} + \frac{l_s\pi}{2}) \cos(\varphi_{ki} + \frac{l_i\pi}{2})]^2 \\ & \quad \times \Theta^2(\Omega_s, k_{s\parallel}, 0, l_s) \Theta^2(\Omega_i, k_{i\parallel}, 0, l_i) U(\Omega_s, k_{s\parallel}) U(\Omega_i, k_{i\parallel}). \end{aligned} \quad (\text{C4})$$

where $C_0 = |\beta|(\gamma P_p d_{\text{eff}})(\pi r_p^2)(\sqrt{\pi} \tau_p)$. Substituting the equation

$$e^{-r_p^2 k_{i\parallel} k_{s\parallel} \cos(\varphi_{ks}-\varphi_{ki})} = \sum_{n=-\infty}^{\infty} (-1)^n I_n(r_p^2 k_{i\parallel} k_{s\parallel}) e^{in(\varphi_{ks}-\varphi_{ki})}, \quad (\text{C5})$$

into Eq. (C4) and implementing the integrals about φ_{ks} and φ_{ki} , we get

$$\begin{aligned} & \sum_{l_s=0,1} \sum_{l_i=0,1} \int d\Omega_s \int d\Omega_i \int d\mathbf{k}_{s\parallel} \int d\mathbf{k}_{i\parallel} |\psi_e(\Omega_s, \Omega_i, \mathbf{k}_{s\parallel}, \mathbf{k}_{i\parallel}, l_s, l_i)|^2 \\ &= \frac{1}{4} \sum_{l_s=0,1} \sum_{l_i=0,1} \int_{-\infty}^{\infty} d\Omega_s \int_{-\infty}^{\infty} d\Omega_i \int k_{s\parallel} dk_{s\parallel} \int k_{i\parallel} dk_{i\parallel} \\ & \quad \times G_\Omega^2(\Omega_s, \Omega_i) g_k^2(k_{s\parallel}, k_{i\parallel}) F_\Omega^2(\Omega_s) F_\Omega^2(\Omega_i) F_k^2(k_{s\parallel}) F_k^2(k_{i\parallel}) \\ & \quad \times I(k_{s\parallel}, k_{i\parallel}, l_s, l_i) \Theta^2(\Omega_s, k_{s\parallel}, 0, l_s) \Theta^2(\Omega_i, k_{i\parallel}, 0, l_i) U(\Omega_s, k_{s\parallel}) U(\Omega_i, k_{i\parallel}), \end{aligned} \quad (\text{C6})$$

where $I(k_{s\parallel}, k_{i\parallel}, l_s, l_i) = (1+r_\chi^2)I_0(r_p^2 k_{s\parallel} k_{i\parallel}) + (1+r_\chi)^2 \cos[(l_s-l_i)\pi] I_2(r_p^2 k_{s\parallel} k_{i\parallel})$. Then the explicit expression of the normalized constant N_a is obtained by $|N_a| = \left(\sum_{l_s=0,1} \sum_{l_i=0,1} \int d\Omega_s \int d\Omega_i \int d\mathbf{k}_{s\parallel} \int d\mathbf{k}_{i\parallel} |\psi_e(\Omega_s, \Omega_i, \mathbf{k}_{s\parallel}, \mathbf{k}_{i\parallel}, l_s, l_i)|^2 \right)^{-1/2}$.

The normalized effective biphoton state is

$$|\psi\rangle_{Ne} = N_a |\psi\rangle_e. \quad (\text{C7})$$

We can get the density matrix of this state as

$$\rho = |N_a|^2 \sum_{l_{s1}=0,1} \sum_{l_{s2}=0,1} \sum_{l_{i1}=0,1} \sum_{l_{i2}=0,1} \int_{-\infty}^{\infty} d\Omega_{s1} \int_{-\infty}^{\infty} d\Omega_{i1} \int_{-\infty}^{\infty} d\Omega_{s2} \int_{-\infty}^{\infty} d\Omega_{i2} \int d^2\mathbf{k}_{s1\parallel} \int d^2\mathbf{k}_{i1\parallel} \int d^2\mathbf{k}_{s2\parallel} \int d^2\mathbf{k}_{i2\parallel}$$

$$\begin{aligned} & \times \psi_e(\Omega_{s1}, \Omega_{i1}, \mathbf{k}_{s1||}, \mathbf{k}_{i1||}, l_{s1}, l_{i1}) \psi_e^*(\Omega_{s2}, \Omega_{i2}, \mathbf{k}_{s2||}, \mathbf{k}_{i2||}, l_{s2}, l_{i2}) \\ & \times a_s^\dagger(\Omega_{s2}, \mathbf{k}_{s2||}, l_{s2}) a_i^\dagger(\Omega_{i2}, \mathbf{k}_{i2||}, l_{i2}) a_s(\Omega_{s1}, \mathbf{k}_{s1||}, l_{s1}) a_i(\Omega_{i1}, \mathbf{k}_{i1||}, l_{i1}) \end{aligned} \quad (C8)$$

Tracing out the parameters $\mathbf{k}_{s1,2||}$, $\mathbf{k}_{i1,2||}$, $l_{s1,2}$ and $l_{i1,2}$ can reduce the density matrix ρ to $\rho_{\omega_s, \omega_i}$ which describes the temporal biphoton state. This process can be presented by the following equation

$$\rho_{\omega_s, \omega_i} = \sum_{l_s=0,1} \sum_{l_i=0,1} \int d\mathbf{k}_{s||} \int d\mathbf{k}_{i||} a_s(\mathbf{k}_{s||}, l_s) a_i(\mathbf{k}_{i||}, l_i) \rho a_s^\dagger(\mathbf{k}_{s||}, l_s) a_i^\dagger(\mathbf{k}_{i||}, l_i). \quad (C9)$$

After that Eq. (C8) is substituted into Eq. (C9) and the commutations

$$\begin{aligned} a_s(\Omega_{s,i}, \mathbf{k}_{s||,i||}, l_{s,i}) a_{s,i}^\dagger(\mathbf{k}'_{s,i||}, l'_{s,i}) &= a_{s,i}(\Omega_{s,i}) \delta(\mathbf{k}_{s||,i||} - \mathbf{k}'_{s,i||}) \delta_{l_{s,i}, l'_{s,i}} + a_{s,i}^\dagger(\mathbf{k}'_{s,i||}, l'_{s,i}) a_{s,i}(\Omega_{s,i}, \mathbf{k}_{s||,i||}, l_{s,i}) \\ a_{s,i}(\mathbf{k}'_{s,i||}, l'_{s,i}) a_{s,i}^\dagger(\Omega_{s,i}, \mathbf{k}_{s||,i||}, l_{s,i}) &= a_{s,i}^\dagger(\Omega_{s,i}) \delta(\mathbf{k}_{s||,i||} - \mathbf{k}'_{s,i||}) \delta_{l_{s,i}, l'_{s,i}} + a_{s,i}^\dagger(\mathbf{k}'_{s,i||}, l'_{s,i}) a_{s,i}(\Omega_{s,i}, \mathbf{k}_{s||,i||}, l_{s,i}) \end{aligned} \quad (C10)$$

are used, the explicit expression of $\rho_{\omega_s, \omega_i}$ can be calculated as

$$\begin{aligned} \rho_{\omega_s, \omega_i} &= |N_a|^2 \sum_{l_s=0,1} \sum_{l_i=0,1} \int_{-\infty}^{\infty} d\Omega_{s1} \int_{-\infty}^{\infty} d\Omega_{i1} \int_{-\infty}^{\infty} d\Omega_{s2} \int_{-\infty}^{\infty} d\Omega_{i2} \int d\mathbf{k}_{s||} \int d\mathbf{k}_{i||} \\ & \times \psi_e(\Omega_{s1}, \Omega_{i1}, \mathbf{k}_{s||}, \mathbf{k}_{i||}, l_s, l_i) \psi_e^*(\Omega_{s2}, \Omega_{i2}, \mathbf{k}_{s||}, \mathbf{k}_{i||}, l_s, l_i) a_s^\dagger(\Omega_{s1}) a_i^\dagger(\Omega_{i1}) a_s(\Omega_{s2}) a_i(\Omega_{i2}) \end{aligned} \quad (C11)$$

Next, the purity $\text{Tr}(\rho_{\omega_s, \omega_i}^2)$ can be obtained as

$$\begin{aligned} \text{Tr}(\rho_{\omega_s, \omega_i}^2) &= \int_{-\infty}^{\infty} d\Omega_s \int_{-\infty}^{\infty} d\Omega_i a_s(\Omega_s) a_i(\Omega_i) \rho_{\omega_s, \omega_i}^2 a_s^\dagger(\Omega_s) a_i^\dagger(\Omega_i) \\ &= |N_a|^2 \sum_{l_{s1}=0,1} \sum_{l_{s2}=0,1} \sum_{l_{i1}=0,1} \sum_{l_{i2}=0,1} \int_{-\infty}^{\infty} d\Omega_{s1} \int_{-\infty}^{\infty} d\Omega_{i1} \int_{-\infty}^{\infty} d\Omega_{s2} \int_{-\infty}^{\infty} d\Omega_{i2} \int d^2\mathbf{k}_{s1||} \int d^2\mathbf{k}_{i1||} \int d^2\mathbf{k}_{s2||} \int d^2\mathbf{k}_{i2||} \\ & \times \psi_e(\Omega_{s1}, \Omega_{i1}, \mathbf{k}_{s1||}, \mathbf{k}_{i1||}, l_{s1}, l_{i1}) \psi_e^*(\Omega_{s1}, \Omega_{i1}, \mathbf{k}_{s2||}, \mathbf{k}_{i2||}, l_{s2}, l_{i2}) \\ & \times \psi_e(\Omega_{s2}, \Omega_{i2}, \mathbf{k}_{s2||}, \mathbf{k}_{i2||}, l_{s2}, l_{i2}) \psi_e^*(\Omega_{s2}, \Omega_{i2}, \mathbf{k}_{s1||}, \mathbf{k}_{i1||}, l_{s1}, l_{i1}) \end{aligned} \quad (C12)$$

Then, after substituting Eqs. (2) and (C1) into Eq. (C12), we obtain

$$\text{Tr}(\rho_{\omega_s, \omega_i}^2) = \frac{B}{|N|^2}, \quad (C13)$$

where $|N| = 1/|N_a|$ and

$$\begin{aligned} B &= \frac{1}{16} \sum_{l_{s1}=0,1} \sum_{l_{s2}=0,1} \sum_{l_{i1}=0,1} \sum_{l_{i2}=0,1} \int_{-\infty}^{\infty} d\Omega_{s1} \int_{-\infty}^{\infty} d\Omega_{i1} \int_{-\infty}^{\infty} d\Omega_{s2} \int_{-\infty}^{\infty} d\Omega_{i2} \int k_{s1||} dk_{s1||} \int k_{s2||} dk_{s2||} \int k_{i1||} dk_{i1||} \int k_{i2||} dk_{i2||} \\ & \times G_{\Omega}^2(\Omega_{s1}, \Omega_{i1}) g_k^2(k_{s1||}, k_{i1||}) F_{\Omega}^2(\Omega_{s1}) F_{\Omega}^2(\Omega_{i1}) F_k^2(k_{s1||}) F_k^2(k_{i1||}) I(k_{s1||}, k_{i1||}, l_{s1}, l_{i1}) \\ & \times G_{\Omega}^2(\Omega_{s2}, \Omega_{i2}) g_k^2(k_{s2||}, k_{i2||}) F_{\Omega}^2(\Omega_{s2}) F_{\Omega}^2(\Omega_{i2}) F_k^2(k_{s2||}) F_k^2(k_{i2||}) I(k_{s2||}, k_{i2||}, l_{s2}, l_{i2}) \\ & \times \Theta^2(\Omega_{s1}, k_{s1||}, 0, l_{s1}) \Theta^2(\Omega_{i1}, k_{i1||}, 0, l_{i1}) U(\Omega_{s1}, k_{s1||}) U(\Omega_{i1}, k_{i1||}) \\ & \times \Theta^2(\Omega_{s1}, k_{s2||}, 0, l_{s2}) \Theta^2(\Omega_{i1}, k_{i2||}, 0, l_{i2}) U(\Omega_{s1}, k_{s2||}) U(\Omega_{i1}, k_{i2||}) \\ & \times \Theta^2(\Omega_{s2}, k_{s1||}, 0, l_{s1}) \Theta^2(\Omega_{i2}, k_{i1||}, 0, l_{i1}) U(\Omega_{s2}, k_{s1||}) U(\Omega_{i2}, k_{i1||}) \\ & \times \Theta^2(\Omega_{s2}, k_{s2||}, 0, l_{s2}) \Theta^2(\Omega_{i2}, k_{i2||}, 0, l_{i2}) U(\Omega_{s2}, k_{s2||}) U(\Omega_{i2}, k_{i2||}). \end{aligned} \quad (C14)$$

The Eq. (C13) is the Eq. (11) in Sec. IV and the Eq. (13) is a compact form of Eq. (C14)

APPENDIX D: CALCULATION OF SPATIAL SCHMIDT NUMBER

To calculate the spatial Schmidt number, the frequency detunings of the signal and idler photons are fixed at Ω_s and Ω_i , respectively. If only the upwardly propagating photons are collected, a spatial biphoton state can be obtained as

$$|\psi\rangle_k = \sum_{l_s=0,1} \sum_{l_i=0,1} \int d\mathbf{k}_{s||} \int d\mathbf{k}_{i||} \psi(\mathbf{k}_{s||}, \mathbf{k}_{i||}, l_s, l_i) a_s^\dagger(\mathbf{k}_{s||}, l_s) a_i^\dagger(\mathbf{k}_{i||}, l_i) |0\rangle_s |0\rangle_i, \quad (D1)$$

where $\psi(\mathbf{k}_{s||}, \mathbf{k}_{i||}, l_s, l_i)$ is the $\psi(\Omega_s, \Omega_i, \mathbf{k}_{s||}, \mathbf{k}_{i||}, j_s, l_s, j_i, l_i)$ in Eq. (3) with fixed Ω_s , Ω_i and $j_{s,i} = 1$. Before further calculation, the state should be normalized, and the normalized factor N_k can be obtained by

$$|N_k|^2 = \frac{1}{\sum_{l_s=0,1} \sum_{l_i=0,1} \int d\mathbf{k}_{s||} \int d\mathbf{k}_{i||} |\psi(\mathbf{k}_{s||}, \mathbf{k}_{i||}, l_s, l_i)|^2}, \quad (D2)$$

With the explicit expression of $\psi(\mathbf{k}_{s||}, \mathbf{k}_{i||}, l_s, l_i)$ obtained from Eq. (3), the denominator at the right hand of Eq. (D2) can be

expressed as

$$\sum_{l_s=0,1} \sum_{l_i=0,1} \int d\mathbf{k}_{s\parallel} \int d\mathbf{k}_{i\parallel} |\psi(\mathbf{k}_{s\parallel}, \mathbf{k}_{i\parallel}, l_s, l_i)|^2 = \frac{1}{4} C_0^2 G_\Omega^2(\Omega_s, \Omega_i) \sum_{l_s=0,1} \sum_{l_i=0,1} \int k_{s\parallel} dk_{s\parallel} \int k_{i\parallel} dk_{i\parallel} g_k^2(k_{s\parallel}, k_{i\parallel}) \times I(k_{s\parallel}, k_{i\parallel}, l_s, l_i) \Theta^2(\Omega_s, k_{s\parallel}, 0, l_s) \Theta^2(\Omega_i, k_{i\parallel}, 0, l_i) U(\Omega_s, k_{s\parallel}) U(\Omega_i, k_{i\parallel}). \quad (D3)$$

where C_0 is the same with that in Eq. (C4) in Appendix C. This expression can give the expression of density matrix of the normalized $|\psi\rangle_k$ as

$$\rho_k = |N_k|^2 \sum_{l_{s1}=0,1} \sum_{l_{i1}=0,1} \sum_{l_{s2}=0,1} \sum_{l_{i2}=0,1} \int d\mathbf{k}_{s1\parallel} \int d\mathbf{k}_{i1\parallel} \int d\mathbf{k}_{s2\parallel} \int d\mathbf{k}_{i2\parallel} \times \psi(\mathbf{k}_{s1\parallel}, \mathbf{k}_{i1\parallel}, l_{s1}, l_{i1}) \psi^*(\mathbf{k}_{s2\parallel}, \mathbf{k}_{i2\parallel}, l_{s2}, l_{i2}) \psi(\mathbf{k}_{s2\parallel}, \mathbf{k}_{i2\parallel}, l_{s2}, l_{i2}) \psi^*(\mathbf{k}_{s1\parallel}, \mathbf{k}_{i1\parallel}, l_{s1}, l_{i1}) \times a_s^\dagger(\mathbf{k}_{s1\parallel}, l_s) a_i^\dagger(\mathbf{k}_{i1\parallel}, l_i) a_s(\mathbf{k}_{s1\parallel}, l_s) a_i(\mathbf{k}_{i1\parallel}, l_i) \quad (D4)$$

Then, the dimensions of $\mathbf{k}_{i\parallel}$, l_s and l_i in ρ_k can be traced to get a reduced density matrix $\rho_{\mathbf{k}_s}$, and the result is

$$\rho_{\mathbf{k}_s} = |N_k|^2 \sum_{l_s=0,1} \sum_{l_i=0,1} \int d\mathbf{k}_{s1\parallel} \int d\mathbf{k}_{s2\parallel} \int d\mathbf{k}_{i\parallel} \psi(\mathbf{k}_{s1\parallel}, \mathbf{k}_{i\parallel}, l_s, l_i) \psi^*(\mathbf{k}_{s2\parallel}, \mathbf{k}_{i\parallel}, l_s, l_i) a_s^\dagger(\mathbf{k}_{s1\parallel}) a_s(\mathbf{k}_{s2\parallel}). \quad (D5)$$

The purity of $\rho_{\mathbf{k}_s}$ is $\text{Tr}(\rho_{\mathbf{k}_s}^2)$ and can be calculated as

$$\text{Tr}(\rho_{\mathbf{k}_s}^2) = \int d\mathbf{k}_{s\parallel} a_s(\mathbf{k}_{s\parallel}) \rho_{\mathbf{k}_s}^2 a_s^\dagger(\mathbf{k}_{s\parallel}). \quad (D6)$$

After that Eq. (D5) is substituted into Eq. (D6), $\text{Tr}(\rho_{\mathbf{k}_s}^2)$ can be expressed as

$$\text{Tr}(\rho_{\mathbf{k}_s}^2) = \frac{T}{N_K^2}, \quad (D7)$$

where $N_K = 1/|N_k|^2$ and

$$T = \sum_{l_{s1}=0,1} \sum_{l_{i1}=0,1} \sum_{l_{s2}=0,1} \sum_{l_{i2}=0,1} \int d\mathbf{k}_{s1\parallel} \int d\mathbf{k}_{s2\parallel} \int d\mathbf{k}_{i1\parallel} \int d\mathbf{k}_{i2\parallel} \times \psi(\mathbf{k}_{s1\parallel}, \mathbf{k}_{i1\parallel}, l_{s1}, l_{i1}) \psi^*(\mathbf{k}_{s2\parallel}, \mathbf{k}_{i1\parallel}, l_{s1}, l_{i1}) \psi(\mathbf{k}_{s2\parallel}, \mathbf{k}_{i2\parallel}, l_{s2}, l_{i2}) \psi^*(\mathbf{k}_{s1\parallel}, \mathbf{k}_{i2\parallel}, l_{s2}, l_{i2}). \quad (D8)$$

Then, it is easy to get the spatial Schmidt number as

$$K_F = 1 / \text{Tr}(\rho_{\mathbf{k}_s}^2) = N_K^2 / T. \quad (D9)$$

According to Eq. (3) in Sec. II, the explicit expression of $\psi(\mathbf{k}_{s\parallel}, \mathbf{k}_{i\parallel}, l_s, l_i)$ can be obtained. After it is substituted into (D8), and the integrals about φ_{ks} and φ_{ki} is implemented, Eq. (D8) can be expressed as

$$T = \sum_{l_{s1}=0,1} \sum_{l_{i1}=0,1} \sum_{l_{s2}=0,1} \sum_{l_{i2}=0,1} \sum_{m_1=0,1} \sum_{m_2=0,1} \sum_{m_3=0,1} \sum_{m_4=0,1} \int k_{s1\parallel} dk_{s1\parallel} \int k_{s2\parallel} dk_{s2\parallel} \int k_{i1\parallel} dk_{i1\parallel} \int k_{i2\parallel} dk_{i2\parallel} \times e^{-\frac{r_p^2(k_{s1\parallel}^2 + k_{s2\parallel}^2 + k_{i1\parallel}^2 + k_{i2\parallel}^2)}{2}} (r_\chi)^{m_1+m_2+m_3+m_4} (F_1 + F_2 + F_3 + F_4 + F_5 + F_6 + F_7 + F_8) \times \Theta(\Omega_s, k_{s1\parallel}, 0, l_{s1}) \Theta(\Omega_s, k_{s2\parallel}, 0, l_{s2}) \Theta(\Omega_s, k_{s2\parallel}, 0, l_{s1}) \Theta(\Omega_s, k_{s1\parallel}, 0, l_{s2}) \times \Theta(\Omega_i, k_{i1\parallel}, 0, 2l_{i1}) \Theta(\Omega_i, k_{i2\parallel}, 0, 2l_{i2}) U(\Omega_s, k_{s1\parallel}) U(\Omega_s, k_{s2\parallel}) U(\Omega_i, k_{i1\parallel}) U(\Omega_i, k_{i2\parallel}), \quad (D10)$$

where

$$F_1 = \frac{1}{16} \cos\left[\frac{(l_{s1} - l_{s2} + m_1 - m_4)\pi}{2}\right] \cos\left[\frac{(l_{s1} - l_{s2} + m_2 - m_3)\pi}{2}\right] \cos\left[\frac{(m_3 - m_4)\pi}{2}\right] \times \cos\left[\frac{(m_1 - m_2)\pi}{2}\right] \sum_{n=-\infty}^{\infty} I_n\left(\frac{r_p^2 k_{s1\parallel} k_{i1\parallel}}{2}\right) I_n\left(\frac{r_p^2 k_{s1\parallel} k_{i2\parallel}}{2}\right) I_n\left(\frac{r_p^2 k_{s2\parallel} k_{i2\parallel}}{2}\right) I_n\left(\frac{r_p^2 k_{s2\parallel} k_{i1\parallel}}{2}\right), \quad (D11)$$

$$F_2 = \frac{1}{128} \cos[(l_{i1} - l_{i2} + m_3 - m_1)\pi] \times \sum_{n=-\infty}^{\infty} I_n\left(\frac{r_p^2 k_{s1\parallel} k_{i1\parallel}}{2}\right) I_{n+2}\left(\frac{r_p^2 k_{s1\parallel} k_{i2\parallel}}{2}\right) I_{n+4}\left(\frac{r_p^2 k_{s2\parallel} k_{i2\parallel}}{2}\right) I_{n+2}\left(\frac{r_p^2 k_{s2\parallel} k_{i1\parallel}}{2}\right), \quad (D12)$$

$$F_3 = \frac{1}{128} \cos[(l_{s1} - l_{s2} - l_{i1} - l_{i2})\pi]$$

$$\times \sum_{n=-\infty}^{\infty} I_n \left(\frac{r_p^2 k_{s1} k_{i1}}{2} \right) I_{n+2} \left(\frac{r_p^2 k_{s1} k_{i2}}{2} \right) I_n \left(\frac{r_p^2 k_{s2} k_{i2}}{2} \right) I_{n+2} \left(\frac{r_p^2 k_{s2} k_{i1}}{2} \right), \quad (D13)$$

$$F_4 = \frac{1}{128} \cos \{ [(l_{s1} + l_{s2} + l_{i1} + l_{i2}) - m_1 - m_2 - m_3 - m_4] \pi \} \\ \times \sum_{n=-\infty}^{\infty} I_n \left(\frac{r_p^2 k_{s1} k_{i1}}{2} \right) I_{n+2} \left(\frac{r_p^2 k_{s1} k_{i2}}{2} \right) I_n \left(\frac{r_p^2 k_{s2} k_{i2}}{2} \right) I_{n+2} \left(\frac{r_p^2 k_{s2} k_{i1}}{2} \right) \quad (D14)$$

$$F_5 = \frac{1}{32} \cos \left[\frac{(l_{s1} + l_{s2} + 2l_{i2} - m_2 - 2m_3 - m_4) \pi}{2} \right] \\ \times \sum_{n=-\infty}^{\infty} I_n \left(\frac{r_p^2 k_{s1} k_{i1}}{2} \right) I_n \left(\frac{r_p^2 k_{s1} k_{i2}}{2} \right) I_{n+2} \left(\frac{r_p^2 k_{s2} k_{i2}}{2} \right) I_n \left(\frac{r_p^2 k_{s2} k_{i1}}{2} \right) \quad (D15)$$

$$F_6 = \frac{1}{32} \cos \left[\frac{(2l_{i1} - 2l_{i2} - m_1 - m_2 + m_3 + m_4) \pi}{2} \right] \\ \times \sum_{n=-\infty}^{\infty} I_n \left(\frac{r_p^2 k_{s1} k_{i1}}{2} \right) I_{n+2} \left(\frac{r_p^2 k_{s1} k_{i2}}{2} \right) I_{n+2} \left(\frac{r_p^2 k_{s2} k_{i2}}{2} \right) I_n \left(\frac{r_p^2 k_{s2} k_{i1}}{2} \right) \quad (D16)$$

$$F_7 = \frac{1}{32} \cos \left[\left(\frac{2l_{s1} + 2l_{s2} - m_1 - m_4 + m_2 + m_3}{2} \right) \pi \right] \\ \times \sum_{n=-\infty}^{\infty} I_n \left(\frac{r_p^2 k_{s1} k_{i1}}{2} \right) I_n \left(\frac{r_p^2 k_{s1} k_{i2}}{2} \right) I_{n+2} \left(\frac{r_p^2 k_{s2} k_{i2}}{2} \right) I_{n+2} \left(\frac{r_p^2 k_{s2} k_{i1}}{2} \right) \quad (D17)$$

$$F_8 = \frac{1}{32} \cos \left[\left(\frac{l_{s1} + l_{s2} + 2l_{i1} - 2m_1 - m_2 - m_4}{2} \right) \pi \right] \\ \times \sum_{n=-\infty}^{\infty} I_n \left(\frac{r_p^2 k_{s1} k_{i1}}{2} \right) I_{n+2} \left(\frac{r_p^2 k_{s1} k_{i2}}{2} \right) I_{n+2} \left(\frac{r_p^2 k_{s2} k_{i2}}{2} \right) I_{n+2} \left(\frac{r_p^2 k_{s2} k_{i1}}{2} \right). \quad (D18)$$

Utilizing Eqs. (D2) and (D9-D18), the spatial Schmidt number of the biphoton state described by Eq. (2) can be calculated numerically. However, a simpler form of (D9) can be derived under two assumptions. Firstly, we only collect the photon pairs with “TE/TE” polarizations. Secondly, pump beam has relatively large transverse radius, so that the signal and idler photon pairs generated in the SpFWM have $\mathbf{k}_{s\parallel} \approx \mathbf{k}_{i\parallel}$. (With this assumption, the term of $G_k(\mathbf{k}_{s\parallel}, \mathbf{k}_{i\parallel}) = e^{-r_p^2(\mathbf{k}_{s\parallel} + \mathbf{k}_{i\parallel})^2/4}$ in Eq. (3) can be simplified as $4\pi\delta(\mathbf{k}_{s\parallel} + \mathbf{k}_{i\parallel})/r_p^2$). After these two assumptions, Eq. (D8) can be simplified to

$$T = \left(\frac{4\pi}{r_p^2} \right)^3 \int d\mathbf{k}_{s\parallel} U(\Omega_s, k_{s\parallel}) U(\Omega_i, k_{s\parallel}). \quad (D19)$$

According to $N_K = 1/|N_k|^2$ and Eq. (D2), a simplified form of N_K can be obtained as

$$N_K = \left(\frac{2\pi}{r_p^2} \right)^2 \left[\int d\mathbf{k}_{s\parallel} U(\Omega_s, k_{s\parallel}) U(\Omega_i, k_{s\parallel}) \right]^2. \quad (D20)$$

With Eqs. (D19) and (D20), an approximated expression of K_F can be obtained as

$$K_F = \frac{1}{8} \frac{\int d\mathbf{k}_{s\parallel} u(\Omega_s, \mathbf{k}_{s\parallel}) u(\Omega_i, -\mathbf{k}_{s\parallel})}{\frac{2\pi}{r_p^2}} \quad (D21)$$

which is the Eq. (18) in Sec. IV.

The biphoton probability amplitude function of the biphoton state generated by SPDC process under the same pump configuration with Fig. 1 (a) can be expressed as [31]

$$\psi(\mathbf{k}_{s\parallel}, \mathbf{k}_{i\parallel}) \propto \tilde{E}_p^{(+)}(\mathbf{k}_{s\parallel} + \mathbf{k}_{i\parallel}) \text{sinc}\left(\frac{\Delta k L}{2}\right) e^{i\frac{\Delta k L}{2}}. \quad (D22)$$

where $\tilde{E}_p^{(+)}(\mathbf{k}_{\parallel})$ is the slowly varying envelope of $E_p^{(+)}(\mathbf{k}_{\parallel})$. Here, the SPDC process is assumed to occur in thick crystal

with longitudinal thickness of L , and the term $\text{sinc}(\Delta kL/2)e^{i\Delta kL/2}$ originates from the longitudinal phase mismatch. After substituting Eq. (A2) into Eq. (D22), and restricting the signal and idler fields to the propagating fields along z axis, we can obtain

$$\psi(\mathbf{k}_{s\parallel}, \mathbf{k}_{i\parallel}) = C_s e^{-\frac{r_p^2 |\mathbf{k}_{s\parallel} + \mathbf{k}_{i\parallel}|^2}{2}} \sin\left(\frac{\Delta kL}{2}\right) e^{i\frac{\Delta kL}{2}} U(\Omega_s, k_{s\parallel}) U(\Omega_i, k_{i\parallel}) \quad (\text{D23})$$

Taking the same process leading to Eqs. (D2), (D8) and (D9), we can get the spatial Schmit number of the SPDC process in thick crystal as

$$\begin{aligned} K_s &= \frac{N_K^2}{T} \int d\mathbf{k}_{s\parallel} \text{sinc}^2(\Delta kL) U(\Omega_s, k_{s\parallel}) U(\Omega_i, k_{i\parallel}) \\ &= \frac{3}{8} \frac{\int d\mathbf{k}_{s\parallel} \text{sinc}^2(\Delta kL) U(\Omega_s, k_{s\parallel}) U(\Omega_i, k_{i\parallel})}{\frac{2\pi}{r_p^2}} \end{aligned} \quad (\text{D22})$$

which is the Eq. (19) in Sec. IV.

APPENDIX E: ESTIMATING THE COINCIDENCE COUNT RATE OF PHOTON PAIR GENERATION

The filtering functions of the signal/idler frequency filters are the same to that shown in Eq. (6.1) in Sec. III, and the filtering functions [38] of the collection system can be approximated by Gaussian functions

$$F_k(\mathbf{k}_s) = e^{-\frac{k_{s\parallel}^2}{2k_s^2 \sin^2 \frac{\theta}{2}}}, \quad F_k(\mathbf{k}_i) = e^{-\frac{k_{i\parallel}^2}{2k_i^2 \sin^2 \frac{\theta}{2}}}, \quad (\text{E1})$$

where $k_{sv} = \omega_s / c$ and $k_{iv} = \omega_i / c$ are the wavenumbers of the signal and idler fields in vacuum. When the frequency filtering bandwidth is not too large, and the central angular frequencies of the signal/idler frequency filters are not far away from ω_{p0} , the filtering functions in Eq. (E1) can be approximated by

$$F_k(\mathbf{k}_s) \approx e^{-\frac{k_{s\parallel}^2}{2k_{p0}^2 \sin^2 \frac{\theta_c}{2}}}, \quad F_k(\mathbf{k}_i) \approx e^{-\frac{k_{i\parallel}^2}{2k_{p0}^2 \sin^2 \frac{\theta_c}{2}}} \quad (\text{E2})$$

Then, the following operators are constructed

$$a_s^\dagger(t_s, \mathbf{r}_s) = (2\pi)^{-\frac{3}{2}} \sum_{l_s=0,1} \int d\Omega_s \int d\mathbf{k}_{s\parallel} a_s^\dagger(\Omega_s, \mathbf{k}_{s\parallel}, 0, l_s) F_\Omega(\Omega_s) F_k(\mathbf{k}_{s\parallel}) e^{i(\mathbf{k}_{s\parallel} \cdot \mathbf{r}_s - \Omega_s t_s)}, \quad (\text{E3})$$

$$a(t_s, \mathbf{r}_s) = (2\pi)^{-\frac{3}{2}} \sum_{l_s=0,1} \int d\Omega_s \int d\mathbf{k}_{s\parallel} a_s(\Omega_s, \mathbf{k}_{s\parallel}, 0, l_s) F_\Omega(\Omega_s) F_k(\mathbf{k}_{s\parallel}) e^{-i(\mathbf{k}_{s\parallel} \cdot \mathbf{r}_s - \Omega_s t_s)}. \quad (\text{E4})$$

Since there is no other source of photons at the signal/idler frequencies in the model shown in Fig. 1 (a), except the photon pairs generated in SpFWM, the signal/idler photon generation rate is equal to the photon pair generation rate[2]. When both of the frequency and spatial frequency filtering functions are uniform for the signal and idler photons, we can get the coincidence count rate by $\eta_i R_s$, where R_s is the single side count rate of signal photon. The expression of R_s is[2]

$$R_s = \eta_s \int d\mathbf{r}_s D(\mathbf{r}_s) \langle \psi | a_s^\dagger(t_s, \mathbf{r}_s) a(t_s, \mathbf{r}_s) | \psi \rangle_{s-i}, \quad (\text{E5})$$

where $D(\mathbf{r}_s) = 1$ ($r_s < r_c$) and $D(\mathbf{r}_s) = 0$ ($r_s > r_c$) are due to the assumption that the single photon detectors have circle aperture with radius of r_c .

Substituting the expression of $|\psi\rangle_{s-i}$ in Eqs. (2) and (3) into Eq. (E5), we can get

$$\begin{aligned} R_s &= (2\pi)^{-3} |\beta|^2 (\gamma P_p d_{\text{eff}})^2 (\sqrt{\pi} \tau_p)^2 (\pi r_p^2)^2 \eta_s \int d\mathbf{r}_s D(\mathbf{r}_s) \\ &\times \langle 0 | \langle 0 | \sum_{l_{s1}=0,1} \sum_{l_{i1}=0,1} \int d\Omega_{s1} \int d\Omega_{i1} \int d\mathbf{k}_{s1\parallel} \int d\mathbf{k}_{i1\parallel} G_\Omega(\Omega_{s1}, \Omega_{i1}) G_k(\mathbf{k}_{s1\parallel}, \mathbf{k}_{i1\parallel}) \\ &\times \Phi(\varphi_{ks1}, \varphi_{ki1}, l_{s1}, l_{i1}) \Theta(\Omega_{s1}, k_{s1\parallel}, 0, l_{s1}) \Theta(\Omega_{i1}, k_{i1\parallel}, 0, l_{i1}) U(\Omega_{s1}, k_{s1\parallel}) U(\Omega_{i1}, k_{i1\parallel}) a_s(\Omega_{s1}, \mathbf{k}_{s1\parallel}, 0, l_{s1}) a_i(\Omega_{i1}, \mathbf{k}_{i1\parallel}, 0, l_{i1}) \\ &\times \sum_{l'_s=0,1} \int d\Omega'_s \int d\mathbf{k}'_{s\parallel} a_s^\dagger(\Omega'_s, \mathbf{k}'_{s\parallel}, 0, l'_s) F_\Omega(\Omega'_s) F_k(\mathbf{k}'_{s\parallel}) e^{-i(\mathbf{k}'_{s\parallel} \cdot \mathbf{r}_s - \Omega'_s t_s)} \\ &\times \sum_{l''_s=0,1} \int d\Omega''_s \int d\mathbf{k}''_{s\parallel} a_s(\Omega''_s, \mathbf{k}''_{s\parallel}, 0, l''_s) F_\Omega(\Omega''_s) F_k(\mathbf{k}''_{s\parallel}) e^{i(\mathbf{k}''_{s\parallel} \cdot \mathbf{r}_s - \Omega''_s t_s)} \\ &\times \sum_{l_{s2}=0,1} \sum_{l_{i2}=0,1} \int d\Omega_{s2} \int d\Omega_{i2} \int d\mathbf{k}_{s2\parallel} \int d\mathbf{k}_{i2\parallel} G_\Omega(\Omega_{s2}, \Omega_{i2}) G_k(\mathbf{k}_{s2\parallel}, \mathbf{k}_{i2\parallel}) \Phi(\varphi_{ks2}, \varphi_{ki2}, l_{s2}, l_{i2}) \end{aligned}$$

$$\times \Theta(\Omega_{s2}, k_{s2||}, 0, l_{s2}) \Theta(\Omega_{i2}, k_{i2||}, 0, l_{i2}) U(\Omega_{s2}, k_{s2||}) U(\Omega_{i2}, k_{i2||}) a_s^\dagger(\Omega_{s2}, \mathbf{k}_{s2||}, 0, l_{s2}) a_i^\dagger(\Omega_{i2}, \mathbf{k}_{i2||}, 0, l_{i2}) |0\rangle |0\rangle. \quad (\text{E6})$$

With the commutations

$$\begin{aligned} [a_s(\Omega_s'', \mathbf{k}_{s||}'', 0, l_s''), a_s^\dagger(\Omega_{s2}, \mathbf{k}_{s2||}, 0, l_{s2})] &= \delta(\Omega_s'' - \Omega_{s2}) \delta(\mathbf{k}_{s||}'' - \mathbf{k}_{s2||}) \delta_{l_s'' l_{s2}} \\ [a_s(\Omega_{s1}, \mathbf{k}_{s||}, 0, l_{s1}), a_s^\dagger(\Omega_s', \mathbf{k}_{s||}', 0, l_s')] &= \delta(\Omega_s' - \Omega_{s1}) \delta(\mathbf{k}_{s||}' - \mathbf{k}_{s||}) \delta_{l_s' l_{s1}} \\ [a_i(\Omega_{i1}, \mathbf{k}_{i||}, 0, l_{i1}), a_i^\dagger(\Omega_{i2}, \mathbf{k}_{i2||}, 0, l_{i2})] &= \delta(\Omega_{i1} - \Omega_{i2}) \delta(\mathbf{k}_{i||} - \mathbf{k}_{i2||}) \delta_{l_{i1} l_{i2}} \end{aligned} \quad (\text{E7})$$

Eq. (E6) can be simplified into

$$\begin{aligned} R_s &= (2\pi)^{-3} |\beta|^2 (\gamma P_p d_{\text{eff}})^2 (\sqrt{\pi} \tau_p)^2 (\pi r_p^2)^2 \eta_s \int d\mathbf{r}_s D(\mathbf{r}_s) \sum_{l_{s1}=0,1} \sum_{l_{s2}=0,1} \sum_{l_{i1}=0,1} \int d\Omega_{s1} \int d\Omega_{s2} \int d\mathbf{k}_{s||} \int d\mathbf{k}_{s2||} \int d\Omega_i \int d\mathbf{k}_{i||} \\ &\times G_\Omega(\Omega_{s1}, \Omega_i) G_k(\mathbf{k}_{s||}, \mathbf{k}_{i||}) G_\Omega(\Omega_{s2}, \Omega_i) G_k(\mathbf{k}_{s2||}, \mathbf{k}_{i||}) \Phi(\varphi_{ks1}, \varphi_{ki}, l_{s1}, l_i) \Phi(\varphi_{ks2}, \varphi_{ki}, l_{s2}, l_i) \\ &\times \Theta(\Omega_{s1}, k_{s1||}, 0, l_{s1}) \Theta(\Omega_{s1}, k_{s1||}, 0, l_{s2}) \Theta^2(\Omega_i, k_{i||}, 0, l_i) U(\Omega_{s1}, k_{s1||}) U(\Omega_{s2}, k_{s2||}) U(\Omega_i, k_{i||}) \\ &\times F_\Omega(\Omega_{s1}) F_k(\mathbf{k}_{s||}) F_\Omega(\Omega_{s2}) F_k(\mathbf{k}_{s2||}) e^{-i(\mathbf{k}_{s||} \cdot \mathbf{r}_s - \Omega_{s1} t_s)} e^{i(\mathbf{k}_{s2||} \cdot \mathbf{r}_s - \Omega_{s2} t_s)}. \end{aligned} \quad (\text{E8})$$

When r_p and τ_p are relatively large, the functions $G_\Omega(\Omega_{s1}, \Omega_i) = e^{-\tau_p^2(\Omega_s^2 + \Omega_i^2)/4}$ and $G_k(\mathbf{k}_{s2||}, \mathbf{k}_{i||}) = e^{-r_p^2(\mathbf{k}_{s2||} + \mathbf{k}_{i||})^2/4}$ can be approximated by $G_\Omega(\Omega_s, \Omega_i) = 2\sqrt{\pi} \delta(\Omega_s - \Omega_i) / \tau_p$ and $G_k(\mathbf{k}_{s||}, \mathbf{k}_{i||}) = 4\pi \delta(\mathbf{k}_{s||} + \mathbf{k}_{i||}) / r_p^2$, respectively. When these approximations are used, Eq. (E8) can be simplified to

$$\begin{aligned} R_s &= 8\pi^3 |\beta|^2 (\gamma P_p d_{\text{eff}})^2 \eta_s \pi r_c^2 \sum_{l_{s1}=0,1} \sum_{l_{s2}=0,1} \sum_{l_{i1}=0,1} \int d\Omega_s \int d\mathbf{k}_{s||} F_\Omega^2(\Omega_s) F_k^2(\mathbf{k}_{s||}) \Phi(\varphi_{ks}, \varphi_{ks} + \pi, l_{s1}, l_i) \Phi(\varphi_{ks}, \varphi_{ks} + \pi, l_{s2}, l_i) \\ &\times \Theta(\Omega_s, k_{s||}, 0, l_{s1}) \Theta(\Omega_s, k_{s||}, 0, l_{s2}) \Theta^2(-\Omega_s, k_{s||}, 0, l_i) U(\Omega_s, k_{s||}) U(\Omega_i, k_{s||}) \end{aligned} \quad (\text{E9})$$

According to Eq. (4.2) and the expression of $U(\Omega_s, k_{s||})$, the terms $\Theta(\Omega_s, k_{s||}, 0, l_{s1})$, $\Theta(\Omega_s, k_{s||}, 0, l_{s2})$, $\Theta^2(-\Omega_s, k_{s||}, 0, l_i)$, $U(\Omega_s, k_{s||})$ and $U(\Omega_i, k_{s||})$ are all nearly unit when the bandwidths of frequency and spatial frequency filtering processes are not very large. In such case, after the expressions of $F_\Omega(\Omega_s)$ and $F_k(\mathbf{k}_{s||})$ in Eq. (6.1) and Eq. (E2) are substituted into Eq. (9), this equation can be simplified to

$$\begin{aligned} R_s &= 8\pi^3 |\beta|^2 (\gamma P_p d_{\text{eff}})^2 \eta_s \pi r_c^2 \sum_{l_{s1}=0,1} \sum_{l_{s2}=0,1} \sum_{l_{i1}=0,1} \int d\Omega_s \int d\mathbf{k}_{s||} F_\Omega^2(\Omega_s) F_k^2(\mathbf{k}_{s||}) \Phi(\varphi_{ks}, \varphi_{ks} + \pi, l_{s1}, l_i) \Phi(\varphi_{ks}, \varphi_{ks} + \pi, l_{s2}, l_i) \\ &= \frac{\pi \sqrt{\pi} n_{p0}^2}{9} (\gamma P_p d_{\text{eff}})^2 \eta_s \Omega_c (k_{p0} r_c \sin \frac{\theta_c}{2})^2 \left[\left(\frac{1 + \gamma_\chi}{2} \right)^2 + \left(\frac{1 - \gamma_\chi}{2} \right)^2 \right], \end{aligned} \quad (\text{E10})$$

With Eq. (E10), the coincidence count per pump pulse can be obtained as $n_c = \eta_i (\sqrt{\pi} \tau_p) R_s$, which is the Eq. (20) in Sec. V.

APPENDIX F: PARAMETERS FOR ESTIMATING THE COINCIDENCE COUNT RATE

Firstly, let us see how to acquire the effective nonlinear interaction length d_{eff} . The losses of the pump light and signal/idler photons along z direction make d_{eff} less than the film thickness. These losses are from the material absorptions, and in the following paragraphs the d_{eff} in different materials will be acquired according to different absorption models.

In Au film, the peak power of the pump light variation along the z direction obeys the equation

$$\frac{dP_p(z)}{dz} = -\alpha_0 - \alpha_T \frac{P_p(z)}{A_{\text{eff}}}, \quad (\text{F1})$$

where α_0 is the linear absorption coefficient and α_T is the two photon absorption (TPA) coefficient, and A_{eff} is the effective area of the pump light. In Eq. (2), we can see that the biphoton probability amplitude is proportional to $P_p d_{\text{eff}}$, in which P_p is the peak power of the pump light before it enters the film. Also, since the signal and idler are weak fields, their decays along z can be described simply by a factor $e^{-\alpha_0 z}$ when α_0 for signal and idler photons are assumed to be the same. Thus, we can define the effective nonlinear interaction length as

$$d_{\text{eff}} = \int_{-d/2}^{d/2} dz e^{-\alpha_0 z} P_p(z) / P_p, \quad (\text{F2})$$

in which $P_p(z)$ can be obtained by numerically solving Eq. (F1).

For layered materials, such as graphene and Bi₂Se₃, the d_{eff} can be defined according to Ref. [38] and has form of

$$d_{eff} = d_L \frac{N_L}{(1 + \frac{N_L}{2} e^{-\alpha_{pL} d_L})^2 (1 + \frac{N_L}{2} e^{-\alpha_{sL} d_L}) (1 + \frac{N_L}{2} e^{-\alpha_{iL} d_L})}, \quad (F3)$$

where d_L , N , and α_{pL} ($\alpha_{sL, iL}$) are the thickness of monolayer, number of layers, and the absorption coefficient of the pump (signal/idler) light in monolayer. The absorption of pump light includes the linear absorption, TPA and saturation absorption (SA).

In graphene, the linear absorption coefficient, TPA coefficient, and the SA threshold of light with wavelength around $1.5\mu m$ are $\alpha_0 = 5.64 \times 10^7 / m$, $\alpha_T = 0.9 \times 10^4 cm / GW$ and $I_{sat} = 3 GW / cm^2$ [39]. In Sec. V, r_p is set as $5\mu m$ and the effective area of the pump light is $A_{eff} = \pi r_p^2$. Under the pump powers used in the calculations about graphene in Sec. V, $\alpha_T P_p / A_{eff}$ is much less than α_0 and the pump light intensity P_p / A_{eff} is lower than I_{sat} . Hence, the TPA and SA effects can be neglected in the calculation of d_{eff} for graphene. In Bi_2Se_3 , according to Ref. [33], even when the incident irradiance at 800nm is $I_{sat} = 10.4 GW / cm^2$, which corresponds to $P_p = 8.16 kW$ with $r_p = 5\mu m$, TPA does not occur. Moreover, the SA threshold of Bi_2Se_3 at 800nm is $I_{sat} = 10.12 GW / cm^2$ and corresponds to $P_p = 7.9 kW$ with $r_p = 5\mu m$, which is much higher than the power used in the calculations about Bi_2Se_3 in Sec. V. Thus, in the calculations about Bi_2Se_3 , the TPA and SA effects also can be neglected. Based on these analysis, Eq. (F3) can be simplified to

$$d_{eff} = d_L \frac{N}{(1 + \frac{N}{2} e^{-\alpha_0 d_L})^4}, \quad (F4)$$

where α_0 is the linear absorption coefficient of graphene/ Bi_2Se_3 . In the derivation of Eq. (F4), α_{sL} and α_{iL} are assumed to be the same.

Secondly, other parameters used in estimating n_c in different materials are listed in the following table.

Table F1 Some parameters used in the calculations for Figs. 5 (a-d)

Au film	Graphene	Bi_2Se_3
$\lambda_p = 600 nm$	$d_L = 0.3 nm$	$d_L = 1 nm$
$\lambda_s = 700 nm$	$\lambda_p = 1530 nm$	$\lambda_p = 800 nm$
$\Omega_c / 2\pi = 1 THz$	$\lambda_s = 1550 nm$	$\lambda_s = 980 nm$
$\theta_c = 6^\circ$	$\Omega_c / 2\pi = 1 THz$	$\Omega_c / 2\pi = 1 THz$
$r_c = 1 mm$	$\theta_c = 6^\circ$	$\theta_c = 6^\circ$
$\chi_{xxxx}^{(3)} = (10^{-17} + i10^{-18}) m^2 / V^2$ [40]	$r_c = 1 mm$	$r_c = 1 mm$
$n_{p0} = 0.24 + i3.07$	$\chi_{xxxx}^{(3)} = 10^{-15} m^2 / V^2$ [38]	$n_2 = 10^{-14} m^2 / W$ [41]
$\alpha_0 = 4.45 \times 10^7 / m$	$n_{p0} = 2.6$	$n_{p0} = 5.5$ [41]
$\alpha_T = 10^{-7} m / W$ [40]	$\alpha_0 = 5.64 \times 10^7 / m$ [38]	$\alpha_0 = 1.38 \times 10^7 / m$ [41]
$r_\chi = 1$	$r_\chi = 1/3$	$r_\chi = 1/3$

-
- | | |
|--|--|
| <p>[1] D. N. Klyshko, Photons and Nonlinear Optics (Gordon and Breach, New York, 1988).</p> <p>[2] C. K. Hong and L. Mandel, Phys. Rev. A 31, 2409 (1985).</p> <p>[3] J. Chen, X. Li, and P. Kumar, Phys. Rev. A 72, 033801 (2005).</p> <p>[4] J. Sharping, K. Lee, M. Foster, A. Turner, B. Schmidt, M. Lipson, A. Gaeta, and P. Kumar, Opt. Express 14, 12388 (2006).</p> <p>[5] Y. Guo, W. Zhang, S. Dong, Y. D. Huang, and J. D. Peng, Opt. Lett. 39, 2526-2529 (2014).</p> <p>[6] J. Zeuner, A. N. Sharma, M. Tillmann, R. Heilmann, M. Gräfe, A. Moqanaki, A. Szameit and P. Walther, Nature 13 1 (2018).</p> <p>[7] R. Ursin, F. Tiefenbacher, T. Schmitt-Manderbach, and etc., Nature Phys. 3, 481–486 (2007).</p> | <p>[8] Q. C. Sun, Y., L., Mao, S. J. Chen and etc., Nat. Photonics 10, 671 (2016).</p> <p>[9] M. H. Rubin, D. N. Klyshko, Y. H. Shih, and A. V. Sergienko, Phys. Rev. A 50, 5122 (1994).</p> <p>[10] A. Gatti, T. Corti, E. Brambilla, and D. B. Horoshko, Phys. Rev. A 86, 053803 (2012).</p> <p>[11] Y. Zhang and F. S. Roux, Phys. Rev. A 89, 063802 (2014).</p> <p>[12] J. Peřina, Jr., Phys. Rev. A 93, 013852 (2016).</p> <p>[13] G. Molina-Terriza, S. Minardi, Y. Deyanova, C. I. Osorio, M. Hendrych, and J. P. Torres, Phys. Rev. A 72, 065802 (2005).</p> <p>[14] O. Jedrkiewicz, M. Clerici, A. Picozzi, D. Faccio, and P. Di Trapani, Phys. Rev. A 76, 033823 (2007).</p> <p>[15] A. Gatti, E. Brambilla, L. Caspani, O. Jedrkiewicz, and L. A. Lugiato, Phys. Rev. Lett. 102, 223601 (2009).</p> |
|--|--|

- [16] O. Jedrkiewicz, A. Gatti, E. Brambilla, and P. Di Trapani, *Phys. Rev. Lett.* 109, 243901 (2012).
- [17] S.W. Du, J. M. Wen, and M. H. Rubin, *J. Opt. Soc. Am. B* 25, C98 (2008).
- [18] J. Monroy-Ruz, K. Garay-Palmett and Alfred B. U'Ren, *New J. Phys.* 18, 103026 (2016).
- [19] M. Barbier, I. Zaquine and P. Delaye, *New J. Phys.* 17, 053031 (2015).
- [20] M. Fiorentino, S. M. Spillane, R. G. Beausoleil, T. D. Roberts, P. Battle, and M. W. Munro, *Opt. Express* 15, 7479-7488 (2007).
- [21] C. I. Osorio, A. Valencia, and J. P. Torres, *New J. Phys.* 10, 113012 (2008).
- [22] M. B. Nasr, B. E. A. Saleh, A. V. Sergienko, and M. C. Teich, *Phys. Rev. Lett.* 91(8), 083601 (2003).
- [23] L. A. Rozema, J. D. Bateman, D. H. Mahler, R. Okamoto, A. Feizpour, A. Hayat, and A. M. Steinberg, *Phys. Rev. Lett.* 112, 223602 (2014).
- [24] K. Garay-Palmett, D. Cruz-Delgado, F. Dominguez-Serna, E. Ortiz-Ricardo, J. Monroy-Ruz, H. Cruz-Ramirez, R. Ramirez-Alarcon, A.B. U'Ren, *Phys. Rev. A*, 93 033810 (2016).
- [25] S. Palomba, S. Zhang, Y. Park, G. Bartal, X. Yin, and X. Zhang, *Nat. Mater.* 11, 34 (2012).
- [26] H. Harutyunyan, R. Beams, and L. Novotny, *Nat. Phys.* 9, 423 (2013).
- [27] B. E. A. Saleh, A. F. Abouraddy, A. V. Sergienko, and M. C. Teich, *Phys. Rev. A* 62, 043816 (2000).
- [28] C. K. Law and J. H. Eberly, *Phys. Rev. Lett.* 92, 127903 (2004).
- [29] W. P. Grice, A. B. U'Ren and I. A. Walmsley, *Phys. Rev. A* 64, 063815 (2001).
- [30] L. Caspani, E. Brambilla, and A. Gatti, *Phys. Rev. A* 81, 033808 (2010).
- [31] A. Gatti, T. Corti, E. Brambilla, and D. B. Horoshko, *Phys. Rev. A* 86, 053803 (2012).
- [32] E. Hendry, P. J. Hale, J. Moger, A. K. Savchenko and S. A. Mikhailov, *Phys. Rev. Lett.* 105, 097401 (2010).
- [33] S. B. Lu, C. J. Zhao, Y. H. Zou, S. Q. Chen, Y. Chen, Y. Li, H. Zhang, S. C. Wen, and D. Y. Tang, *Opt. Express* 21, 2072 (2013).
- [34] M. Currie, J. D. Caldwell, F. J. Bezares, J. Robinson, T. Anderson, H. Chun, and M. Tadjer, *App. Phys. Lett.* 99, 211909 (2011).
- [35] J. Krüger, D. Dufft, R. Koter, and A. Hertwig, *App. Surf. Sci.* 253, 7815 (2007).
- [36] M. Atatüre, G. Di Giuseppe, M. D. Shaw, A. V. Sergienko, B. E. A. Saleh, and M. C. Teich, *Phys. Rev. A* 65, 023808 (2002); M. Atatüre, G. Di Giuseppe, M. D. Shaw, A. V. Sergienko, B. E. A. Saleh, and M. C. Teich, *Phys. Rev. A* 66, 023822 (2002).
- [37] J. W. Goodman, *Introduction to Fourier Optics*, 3rd edn, Roberts & Company, Englewood Colorado (2005).
- [38] S. A. Mikhailov, *Phys. E* 44 924 (2012); C. Q. Xia, C. Zheng, M. S. Fuhrer, and S. Palomba, *Opt. Lett.* 41, 1122 (2016).
- [39] G. Demetriou, H. T. Bookey, F. Biancalana, E. Abraham, Y. Wang, W. Ji, and A. K. Kar, *Opt. Express* 24, 13033 (2016).
- [40] R. W. Boyd, Z. Shi, I. De Leon, *Opt. Commun.* 326, 74 (2014).
- [41] J. W. McIver, D. Hsieh, S. G. Drapcho, D. H. Torchinsky, D. R. Gardner, Y. S. Lee, and N. Gedik, *Phys. Rev. B* 86, 035327 (2012).